

**NAVAL POSTGRADUATE SCHOOL**  
**Monterey, California**



19980611 007

**THESIS**

**A P-VECTOR APPROACH TO  
ABSOLUTE GEOSTROPHIC CURRENTS IN THE  
ADRIATIC SEA**

by

Renato Lima Pinto

March 1998

Thesis Advisor:  
Second Reader:

Pierre-Marie Poulain  
Peter Chu

**Approved for public release; distribution is unlimited**

# REPORT DOCUMENTATION PAGE

Form Approved  
OMB No. 0704-0188

Public reporting burden for this collection of information is estimated to average 1 hour per response, including the time for reviewing instruction, searching existing data sources, gathering and maintaining the data needed, and completing and reviewing the collection of information. Send comments regarding this burden estimate or any other aspect of this collection of information, including suggestions for reducing this burden, to Washington headquarters Services, Directorate for Information Operations and Reports, 1215 Jefferson Davis Highway, Suite 1204, Arlington, VA 22202-4302, and to the Office of Management and Budget, Paperwork Reduction Project (0704-0188) Washington DC 20503.

<b>1. AGENCY USE ONLY (Leave blank)</b>		<b>2. REPORT DATE</b> March 1998	<b>3. REPORT TYPE AND DATES COVERED</b> Master's Thesis	
<b>4. TITLE AND SUBTITLE</b> A P-vector Approach to Absolute Geostrophic Currents in the Adriatic Sea			<b>5. FUNDING NUMBERS</b>	
<b>6. AUTHOR(S)</b> Renato Lima Pinto			<b>8. PERFORMING ORGANIZATION REPORT NUMBER</b>	
<b>7. PERFORMING ORGANIZATION NAME(S) AND ADDRESS(ES)</b> Naval Postgraduate School Monterey, CA 93943-5000			<b>10. SPONSORING / MONITORING AGENCY REPORT NUMBER</b>	
<b>9. SPONSORING / MONITORING AGENCY NAME(S) AND ADDRESS(ES)</b>			<b>11. SUPPLEMENTARY NOTES</b> The views expressed in this thesis are those of the author and do not reflect the official policy or position of the Department of Defense or the U.S. Government.	
<b>12a. DISTRIBUTION / AVAILABILITY STATEMENT</b> Approved for public release; distribution is unlimited.			<b>12b. DISTRIBUTION CODE</b>	
<b>13. ABSTRACT (maximum 200 words)</b> With the recent conflict in Bosnia-Herzegovina being in the world news front, the Adriatic Sea has become an important strategic operating area for the North Atlantic Treaty Organization (NATO) and for the US Navy. The NATO Undersea Research Centre located in La Spezia, Italy carried out the Otranto Gap (OGAP) project in 1994 and 1995 to assess the oceanography and bottom geology of the Southern Adriatic. As part of this project, the OGEX1 cruise was conducted between 19 and 24 May 1995 with focus in the Otranto Strait, through which the Adriatic is connected to the rest of the Mediterranean basin, and on the Albanian shelf. In this thesis the water masses present in the southern Adriatic are studied and the P-vector method is used to estimate the absolute geostrophic circulation, based on the hydrographic data (CTD, XCTD and XBT) collected during the OGEX1 cruise. The P-vector results are interpreted and compared with other oceanographic data sets acquired during the OGAP project, namely, current meter and ADCP data, drifter tracks and thermal satellite images. The absolute geostrophic velocity at 40 m, derived by the P-vector method, shows rather well the expected cyclonic circulation in the Southern Adriatic north of 41°N. In contrast, the results in the Otranto Strait area need to be interpreted with caution. Current meter data show that this area is very ageostrophic. A comparison between geostrophic and directly measured vertical velocity shears indicates a large departure from geostrophy in this area. The wind is shown to be a main factor forcing the circulation in the Adriatic, either directly or through changes in sea level.				
<b>14. SUBJECT TERMS</b> Oceanographic Survey, P-Vector Method to calculate Absolute Geostrophic Currents, Mooring, ADCP, Floats and Drifters.			<b>15. NUMBER OF PAGES</b> 91	
<b>17. SECURITY CLASSIFICATION OF REPORT</b> Unclassified			<b>16. PRICE CODE</b>	
<b>18. SECURITY CLASSIFICATION OF THIS PAGE</b> Unclassified		<b>19. SECURITY CLASSIFICATION OF ABSTRACT</b> Unclassified		<b>20. LIMITATION OF ABSTRACT</b> UL

NSN 7540-01-280-5500

Standard Form 298 (Rev.289)  
Prescribed by ANSI Std. 239-18



Approved for public release; distribution is unlimited

**A P-VECTOR APPROACH TO ABSOLUTE GEOSTROPHIC CURRENTS IN THE  
ADRIATIC SEA**

Renato Lima Pinto  
Lieutenant, Brazilian Navy  
B.S., Universidade Federal do Rio de Janeiro, 1981

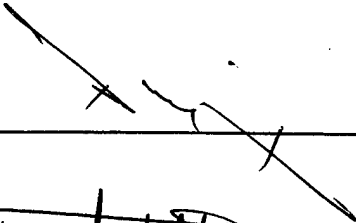
Submitted in partial fulfillment of the  
requirements for the degree of

**MASTER OF SCIENCE IN PHYSICAL OCEANOGRAPHY**

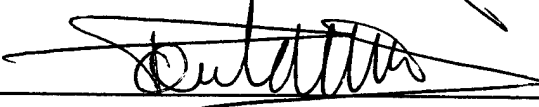
from the

**NAVAL POSTGRADUATE SCHOOL  
March 1998**

Author:

  
\_\_\_\_\_

Approved by:

  
\_\_\_\_\_

Pierre-Marie Poulain, Thesis Advisor

  
\_\_\_\_\_

Peter Chu, Second Reader

  
\_\_\_\_\_

Robert H. Bourke, Chairman  
Department of Oceanography



## ABSTRACT

With the recent conflict in Bosnia-Herzegovina being in the world news front, the Adriatic Sea has become an important strategic operating area for the North Atlantic Treaty Organization (NATO) and for the US Navy. The NATO Undersea Research Centre located in La Spezia, Italy carried out the Otranto Gap (OGAP) project in 1994 and 1995 to assess the oceanography and bottom geology of the Southern Adriatic. As part of this project, the OGEX1 cruise was conducted between 19 and 24 May 1995 with focus in the Otranto Strait, through which the Adriatic is connected to the rest of the Mediterranean basin, and on the Albanian shelf. In this thesis the water masses present in the southern Adriatic are studied and the P-vector method is used to estimate the absolute geostrophic circulation, based on the hydrographic data (CTD, XCTD and XBT) collected during the OGEX1 cruise. The P-vector results are interpreted and compared with other oceanographic data sets acquired during the OGAP project, namely, current meter and ADCP data, drifter tracks and thermal satellite images. The absolute geostrophic velocity at 40 m, derived by the P-vector method, shows rather well the expected cyclonic circulation in the Southern Adriatic north of  $41^{\circ}\text{N}$ . In contrast, the results in the Otranto Strait area need to be interpreted with caution. Current meter data show that this area is very ageostrophic. A comparison between geostrophic and directly measured vertical velocity shears indicates a large departure from geostrophy in this area. The wind is shown to be a main factor forcing the circulation in the Adriatic, either directly or through changes in sea level.



## TABLE OF CONTENTS

I.	INTRODUCTION . . . . .	.1
II.	BACKGROUND . . . . .	3
	A. BATHYMETRY . . . . .	3
	B. WEATHER . . . . .	5
	C. CIRCULATION AND WATER MASSES . . . . .	6
III.	DATA . . . . .	13
	A. OGEX1 CRUISE . . . . .	13
	B. HYDROGRAPHIC SURVEY (CTD, XCTD and XBT) . . . . .	14
	C. MOORING DEPLOYMENTS . . . . .	16
	D. FLOAT AND DRIFTER DEPLOYMENTS . . . . .	18
	E. ADCP (ACOUSTIC DOPPLER CURRENT PROFILER) . . . . .	18
	F. SATELLITE IMAGES . . . . .	18
	G. METEOROLOGICAL DATA . . . . .	19
IV.	P-VECTOR METHOD . . . . .	21
	A. INTRODUCTION . . . . .	21
	B. THERMAL WIND RELATION. . . . .	22
	C. CONSERVATION PRINCIPLES. . . . .	22
	D. P-VECTOR FIELD . . . . .	23
	E. SOURCES OF ERROR . . . . .	25
	F. MAXIMUM TURNING ANGLE PRINCIPLE . . . . .	25
	G. ERROR REDUCTION SCHEME . . . . .	26
V.	RESULTS . . . . .	29
	A. HYDROGRAPHIC DATA ANALYSES . . . . .	29
	B. GEOSTROPHIC CIRCULATION MAPS. . . . .	37
	1. Relative Geostrophic Maps . . . . .	37
	2. P-vector Sections . . . . .	37
	C. MOORED CURRENT METER AND DRIFTER DATA . . . . .	48
	1. Moored Current Meter Data Time Series . . . . .	48
	2. Moored Current Meter Velocities and Drifter Paths . . . . .	55

VI. DISCUSSION . . . . .	59
A. P-VECTOR ABSOLUTE GEOSTROPPHIC FLOW AND MOORING VELOCITIES . . . . .	59
B. P-VECTOR NORTHWARD ABSOLUTE GEOSTROPHIC FLOW VERSUS NORTHWARD CURRENT METER VELOCITIES . . . . .	60
C. P-VECTOR ABSOLUTE GEOSTROPHIC CURRENTS VERSUS ADCP AND AVHRR MAPS. . . . .	65
VII. CONCLUSIONS AND RECOMMENDATIONS . . . . .	.71
A. CONCLUSIONS . . . . .	.71
B. RECOMMENDATIONS . . . . .	.72
LIST OF REFERENCES . . . . .	.75
INITIAL DISTRIBUTION LIST . . . . .	79

## ACKNOWLEDGEMENTS

I would like to offer my sincere appreciation to many people who have provided moral and scientific support. My advisors Dr. Pierre-Marie Poulain for the suggestions and ideas and Dr. Peter Chu for letting me test the P-vector method in a very hostile environment. The NATO SACLANT Undersea Research Centre, La Spezia Italy for making the data available.

Mostly important, I would like to thank God for giving me the opportunity of successfully finish my Master degree. My parents for giving life and love. My wife Gloria, my two children Rachel and Guilherme, and my niece Fernanda, who have survived patiently and endured the many long days and nights in the two years as a student at NPS. Finally I would like to thank my friends Jose Eduardo and Mike Cook for the enormous patience in the FORTRAN and MATLAB coding and Dr. Robert Haney for precious moments on teaching me something about ageostrophy.

## I. INTRODUCTION

Knowledge of the ocean circulation in strategic operational areas is of great importance to undersea and mine warfare. With the recent conflict in Bosnia-Herzegovina being in the world news forefront, the Adriatic Sea has become quite an important place for the North Atlantic Treaty Organization (NATO) and for the US Navy. The "Otranto Gap" project (OGAP) was undertaken by NATO in 1994 and 1995 to study the oceanography and the bottom geology of the southern Adriatic with main focus on the Otranto Strait, through which the Adriatic is connected to the rest of the Mediterranean Sea, and on the Albanian shelf. The oceanographic milestone of OGAP was the OGEX1 cruise conducted in May 1995. The hydrographic data (CTD, XCTD and XBT) collected during OGEX1 is used in this thesis to study the water masses and to estimate the absolute geostrophic circulation via the P-vector method. The results are interpreted and compared to other oceanographic data sets acquired as part of the OGAP project, namely current meter and Acoustic Doppler Current Profiler (ADCP) data, drifter tracks and satellite thermal images. The existence of these extensive contemporaneous data sets provide us the initial impetus to assess the validity of the P-vector method in the coastal environment of the Adriatic Sea.

This thesis is divided into seven Chapters. Chapter II reviews the Adriatic Sea circulation and the components that most affect its patterns. The OGEX1 cruise as well as the data collected are discussed in Chapter III. In Chapter IV the P-vector method is explained. The hydrographic data and the P-vector results are presented in Chapter V along with contemporaneous current meter, ADCP and drifter measurements. Chapter VI includes the comparison between the P-vector estimates and other direct measurements of velocity. Conclusions and

recommendations for follow-on studies are presented in Chapter VII.

## II. BACKGROUND

This Chapter describes the major bathymetric features, the weather patterns and the circulation of the Adriatic Sea. The manner in which they are related to each other and how they affect the circulation pattern is also presented.

### A. BATHYMETRY

The Adriatic Sea (Fig. 1) is an elongated (783 km long) semi-enclosed ocean basin, having an average width of 243 km. It is commonly divided into three areas, north, middle and south.

The northern Adriatic is very shallow with an average depth of only 70 m. A smooth bottom gradually slopes to 100 m and then quickly deepens to 200 m near Ancona, Italy (Orlic et al., 1992).

The middle part of the Adriatic begins immediately south of Ancona, Italy and ends at the Palagruzza Sill, a shoal area with a maximum depth of 170 m immediately west of Dubrovnik. The Jabuka Pit, a 280 m deep depression, is the prominent bottom topographic feature in this area.

The southern Adriatic is steep-sided with a maximum depth of 1233 m found in its center. It starts at the Palagruzza Sill to the north and ends at the Adriatic Sea entrance, the Otranto Strait. The central depth is known as the South Adriatic Pit. Its bottom is a smooth, abyssal plain consisting of clay and mud with an average depth of 1200 m (Buljan and Zore-Armanda, 1976).

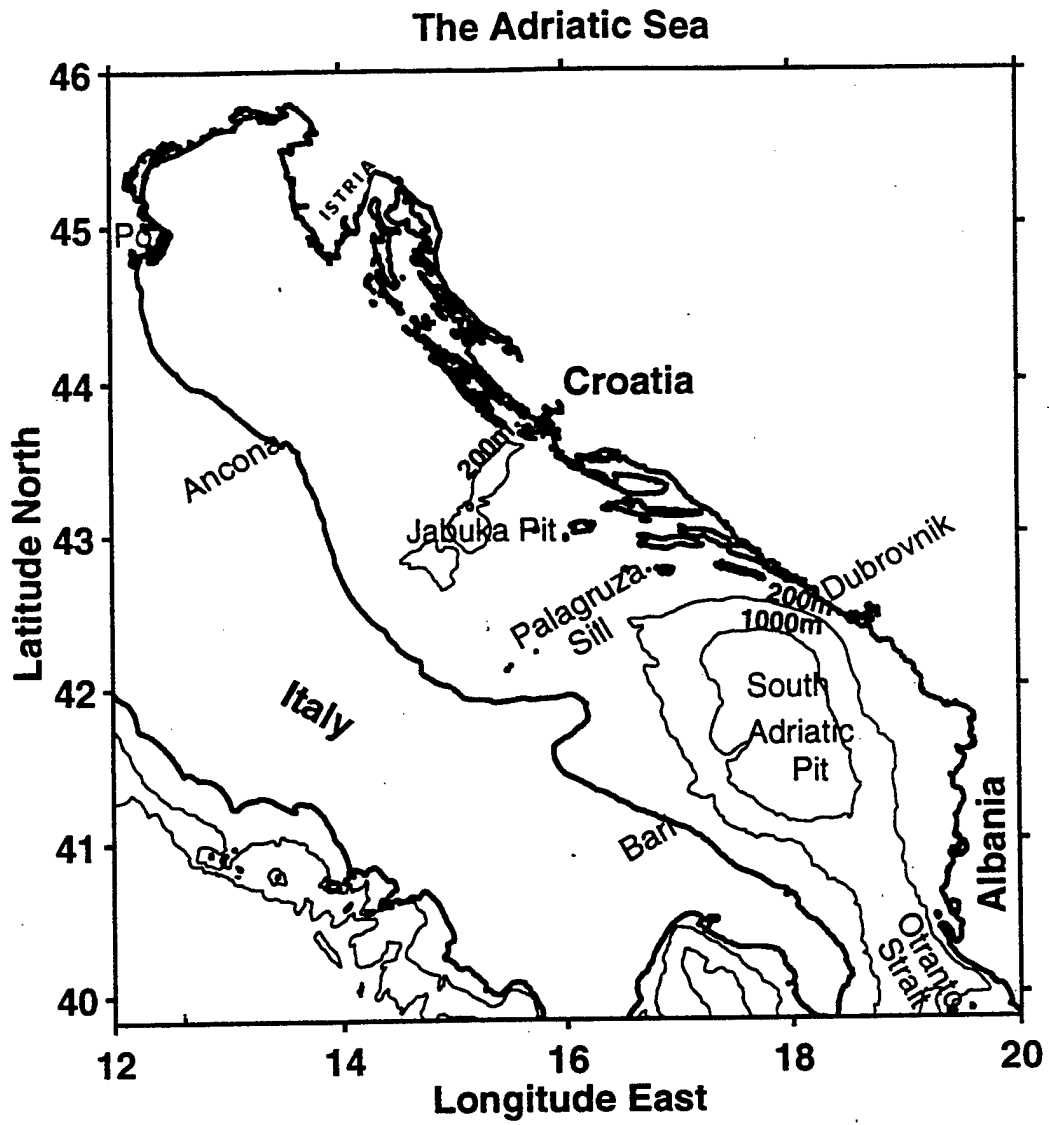


Figure 1: Adriatic Sea geography and bathymetry

A short continental shelf transition zone off both coasts connects to a steep continental slope. Minimal sediment exists in this region due to strong turbidity currents (Buljan and Zore-Armanda, 1976). Islands abruptly rise all along the rugged eastern coastline of the Adriatic while regular isobaths parallel the western shore.

The Otranto Strait shoals from the deeper South Adriatic Pit to a maximum sill depth of 800 m before again plummeting to the deeper Ionian Sea. The mean depth of the strait is 325 m and the width is 75 km (Gacic et al., 1996).

## **B. WEATHER**

Since it is a semi-enclosed basin, the Adriatic Sea is strongly influenced by meteorological conditions. Rugged, mountainous coastlines in the north and east enhance wind effects on the sea surface. The basin is situated between the subtropical high pressure zone and the mid-latitude or westerly belt. Generally, weather systems are dominated by the mid-latitude belt. However, a summer subtropical high pressure zone subverts the westerlies dissipating most disturbances. Mesoscale atmospheric events such as local winds, gravity waves, etc. may modify the regional weather patterns on time scales ranging from a few days to a week (Orlic et al., 1992).

Northeasterly dry winds, known as Bora, can be quite strong (gusts up to 50 m/s) and mostly occur in winter. The southeasterly Sirocco winds also dominate the winter months. Northwesterly Etesian winds blow during the summer months, especially in the south where 53% of all winds are Etesian. Summer air temperatures range between 22-26 °C. In the winter the range is from an average of 2 °C in the north to an average of 10 °C in the south (Orlic et al., 1992). Maximum and minimum precipitation occurs during late fall and summer months, respectively. The inland precipitation is 1000 mm/yr while along

the coast is around 400 mm/yr. The large inland precipitation enhances the importance of river runoff to the general circulation (Orlic et al., 1992).

### C. CIRCULATION AND WATER MASSES

The general circulation of the Adriatic Sea is rather complex. Overall, the general surface circulation is represented by a basin-wide cyclonic (anti-clockwise) gyre with northward flow along the eastern portion of the Adriatic and southward flow along the western coast. A wide current on the eastern side dominates the summer months (Orlic et al., 1992). Smaller cyclonic gyres exist in each of the three Adriatic subsections (Zore, 1956; Poulain, 1998). Topography influences the flow, especially around the Jabuka and South Adriatic Pits. Seasonal variations in the wind and river runoff as well as high frequency wind forcing and density-driven currents, seiche oscillations and tides all disturb the mean flow.

High frequency winds normally intensify the mean surface flow. Gacic et al. (1996, page 136) write "The north current and the same wind velocity component are well correlated in the coastal areas, suggesting that the wind blowing along the Otranto Strait axis generates a downward current in the vicinity of the boundaries". However, if strong abnormal winds prevail, the winds can also decrease or even reverse the mean surface flow, (Poulain, 1998). Mesoscale features created by instability of the strong mean shear flow would then prevail. During a related drifter project, the response to high frequency events was shown by meandering drifters in the areas of normally high speed currents (Gacic et al., 1996; Poulain, 1998).

Tracks of Lagrangian drifters highlighted upwelling areas in the southern Adriatic (Poulain, 1998). Created by local north and northeasterly winds, these upwelling events modify the general current pattern causing the drifters to meander rather than

follow the normal circulation pattern. Strong, short duration local winds can also reverse the general flow, although this is very intermittent and rather rare (Gacic et al., 1996; Poulain, 1998).

Tidal currents are generally not substantial, except near the head of the Adriatic basin with observed amplitudes of 15 cm/s (Buljan and Zore-Armanda, 1976). The diurnal tidal amplitudes increase from the southeast to northwest along the basin. Tides are of the mixed type. Being an order of magnitude larger than the minor axes, the tidal ellipse major axes are aligned parallel with the shoreline. The tidal current vectors generally rotate cyclonically (Orlic et al., 1992). In the southern Adriatic the amplitudes are relatively small, being less than 5 cm/s (Brauns, 1997).

In the northern Adriatic, surface winds can exert a strong influence in forcing the currents. Transient currents, an order of magnitude larger than the mean currents, can be generated (Poulain, 1998). The most notable are the strong Bora winds. Blowing over the shallow northern Adriatic during the winter months, these frigid, dry winds cool the entire water column. A cold less saline, dense water mass, North Adriatic Water (NAW) (Table I), is created by the rapid cooling and evaporation of the water column in addition to mixing from the cold Po River outflow. A thermal front is established between the cold, less saline waters and the warmer and more saline waters advected from the south along the eastern coast. The position of the front varies with the strength and the frequency of the Bora winds. Strong prolonged Bora winds produce a zonal front stretching from the Istria Peninsula tip westward (Fig. 1). Weaker wind events generate an alongshore front parallel to the Italian coast near the Po River delta. Perceived convergence at the frontal zone indicates that the front is the formation site for the NAW (Zore-

Armanda and Gacic, 1987). The severity of the winter dictates the amount and the characteristics of the NAW.

Horizontal density gradients induced by these buoyancy fluxes and the coastal fresh water input explain the horizontal cyclonic flow. Due to temperature differences in the winter months, meridional and zonal density gradients develop. The steric height slope along with recurrent episodes of the southeasterly Sirocco wind generates a stronger, northward flow along the eastern boundary (Orlic et al., 1992). During the summer months the northern Adriatic waters are warmer and less saline than the middle Adriatic waters. In conjunction with the northwesterly Etesian winds, this explains the stronger southward flow along the west coast (Zore, 1956).

As stated previously, the Po River also influences the circulation. Maximum runoff occurs in the fall following heavy precipitation and in the spring after the snow melts. The annual mean runoff from the Po River is 1700 m<sup>3</sup>/s (Orlic et al., 1992). The strong winter Bora winds confine the river's runoff to the Italian Coast while the runoff penetrates to the middle portion of the northern Adriatic in the summer months. No other rivers flow into the Adriatic along the northern or western coasts. Rivers along the east coast supply an annual mean runoff of 1150 m<sup>3</sup>/s along the Albanian coast (Orlic et al., 1992). Seasonal modifications to the freshwater influx dramatically alter the mean flow as seen by the strong intensification of the general cyclonic circulation during the higher freshwater influx periods (winter) and significantly weaker during the lower influx periods (summer). These variations occur at low frequency, on the order of once per month.

After its formation the NAW sinks and flows along the western side of the Adriatic in a narrow vein. Some of the water spills into the Jabuca Pit in the middle Adriatic. It remains there until another pulse of NAW displaces the water, causing it to

flow into the South Adriatic Pit. Thus, the NAW flow is highly dependent on the meteorological conditions (Buljan and Zore-Armanda, 1976). The bulk of the water mass continues along the Italian coast until reaching the southern Adriatic.

Winter cooling and the presence of the Sirocco winds drives the formation of the Adriatic Deep Water (ADW) (Table I). ADW is also known as South Adriatic Water (SAW) (Orlic et al., 1992). The discussion concerning the relationship between the NAW and ADW has three arguments. The first states that the mixing with the Modified Levantine Intermediate Water (MLIW) (Table I) with a core at about 200 m in the South Adriatic Pit creates the ADW (Zoccolatti and Salusti, 1987). The second opinion is that the ADW overlays the NAW with little mixing occurring (Ovchinnikov, 1985). Thirdly, some theoreticians state that occasional mixing occurs near the South Adriatic Pit (Zore-Armanda, 1963). All theories agree that the ADW flows out through the Otranto Strait eventually forming the Eastern Mediterranean Deep Water (EMDW) (Orlic et al., 1992). Recent current measurements (Poulain et al., 1996) revealed that this outflow is intermittent with a periodicity of about 10 days.

A fourth body of water found in the Adriatic Sea is the Middle Adriatic Water (MAW) (Table I). It is not as distinct as the other water masses, in fact it has not been reported by investigators other than Zore-Armanda (Orlic et al., 1992), who states that the MAW is formed in the Jabuka Pit area during periods of weak Mediterranean inflow.

Surface waters are also defined. The western boundary surface layer is composed of diluted outflowing water. This water mass is the Adriatic Surface Water (ASW). Being primarily composed of the Po River runoff, the characteristics of this water mass vary with the season. Late spring and early summer runoffs produce a strong, broader outflow through the Otranto Strait during the summer months (Zore, 1956; Poulain, 1998). The

relatively warm and salty Ionian Surface Water (ISW) is found on the eastern flank of the Otranto Strait.

Table I: Characteristics of the water masses in the Adriatic Sea (from Orlic et al., 1992).

WATER MASS	T(°C)	S(PSU)	Sigma-t
NAW(*)	11	38.5	29.52
ADW	13	38.6	29.20
MLIW	>14.7	>38.7	29.06
MAW(*)	12	38.2	29.09
ASW	<13	<38.2	-
ISW	>15	>38.3	-

(\*) Not present in southern Adriatic.

With large outflow occurring in the deep layers and on the western confines of the Strait in the surface layer, an inflow from the Ionian Sea must be present to compensate. This inflowing water is generally warmer and more saline, flowing in the surface layers predominately on the eastern portion of the Strait. The inflow is seasonally altered as noted by Lagrangian drifters deployed in the Otranto Strait (Poulain, 1998). In spring, small mesoscale features dominate, demonstrating weak surface currents in and out of the area. The fall and to a lesser extent the winter months exhibit a strong, broad persistent inflow on the eastern side of the Strait. A narrow outflow of water exists on the western coastline and into the middle of the Strait. The opposite occurred during the summer months (Poulain, 1998).

The MLIW flows into the Adriatic Sea at intermediate levels on the eastern flank of the Otranto Strait. It originates from the eastern Mediterranean in the Levantine Basin. Warm dry air

evaporates the water creating this warm, saline water mass. As it circulates into the Ionian Sea, it descends to intermediate depths with a core located at approximately 200 m (Orlic et al., 1992). No seasonal variations in this water mass have been observed. However, long-term water mass differences and their influence on the entire circulation have been noted (Gacic et al., 1996). Fig. 2 shows a schematic representation of the Adriatic water types and the typical fluxes through the Otranto Strait for summer and winter.

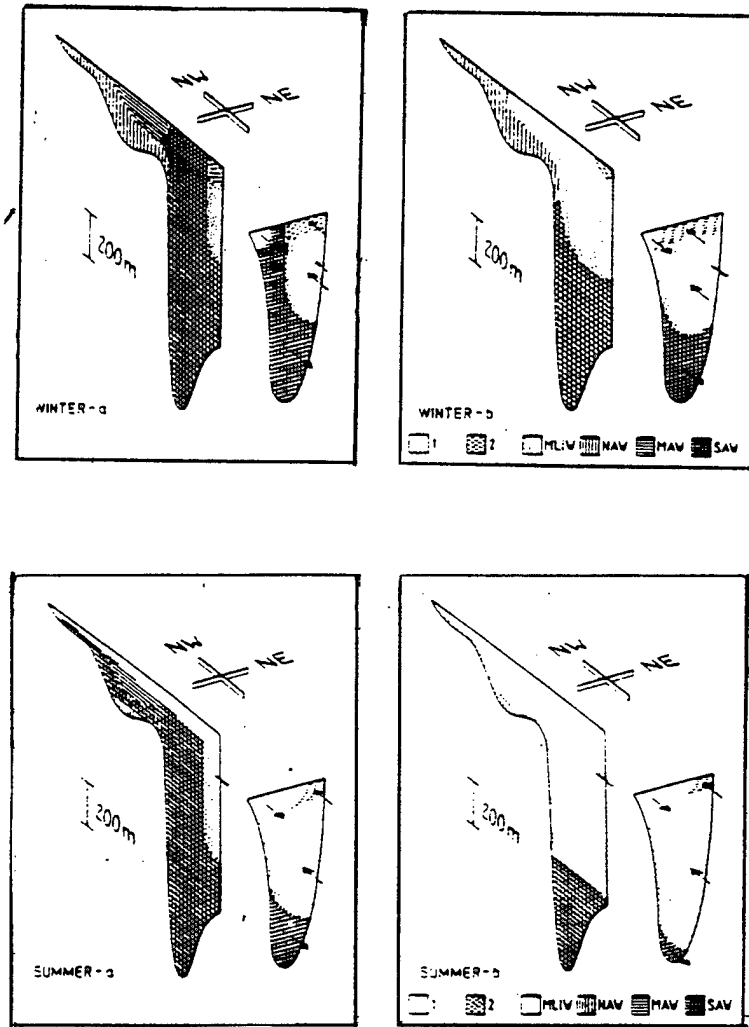


Figure 2: Schematic representation of surface currents and water types of the Adriatic during winter (top) and summer (bottom) with a) lower and b) higher inflow of high-salinity waters. Numbers 1 and 2 denote surface waters, whereas letters denotes water types (from Orlic et al., 1992).

### III. DATA

#### A. OGEX1 CRUISE

As previously stated, the OGEX1 cruise was the main part of the Otranto Gap Project whose objectives were to rapidly assess the oceanographic parameters and seafloor characteristics of the Otranto Gap area. The OGEX1 cruise was carried out by the NATO SACLANT Undersea Research Centre, La Spezia, Italy (SACLANTCEN).

The main purpose of the OGEX1 cruise was to understand the water mass properties and its influence on the general Adriatic circulation, necessary for the successful conduct of mine and anti-submarine warfare.

The specific objectives of the OGEX1 cruise (Poulain, 1995, page 2) were:

1. To conduct a rapid assessment survey in the Otranto Strait with particular focus on the Albanian Coast, including high resolution hydrography with CTD casts (temperature, salinity, dissolved oxygen and turbidity measurements), shipboard ADCP, surface meteorology and shipborne remote sensing).

2. To deploy moorings with current meters, and an ADCP at key locations in the Strait and in the southern Adriatic in order to monitor the exchange of water masses between the Ionian and Adriatic basins.

3. To test the feasibility of following intermediate waters with autonomous (ALACE, MARVOR and drogued drifter) systems in a regional sea environment, i.e., tracking of the MLIW in the southern Adriatic.

4. To release surface drifters to measure the surface circulation and the sea surface temperature in the eastern Otranto Gap and southern Adriatic.

5. To acquire and process SST satellite images in near-real time.

6. To prove the concept of integration of hydrographic data (CTD, XCTD and XBT into the onboard Geographical Information System, and carry out ship-to-ship transfers of analyzed data in near real-time.

The cruise took place between 12 and 24 May 1995 in the Otranto Strait and in the southern Adriatic in the region bounded by 41° 30'N and 39° 45'N and 17°E and 20°E.

Four ships participated in the OGEX1 cruise:

1. NRV Alliance: Hydrography (CTD, XCTD and XBT), ADCP, mooring deployments, floats and surface drifters, remote sensing, surface meteorology
2. ITS Magnaghi: Hydrography (CTD and XBT)
3. ITS Urania: Hydrography (CTD and XBT)
4. HS Nautilus: Surface drifters

#### **B. HYDROGRAPHIC SURVEY**

The hydrographic sections traversed by the NRV Alliance, ITS Magnaghi and ITS Urania are depicted in Fig. 3. NRV Alliance was equipped with a WOCE MK-III CTD, a Beckam dissolved oxygen meter, a Sea Tech 25-cm-path transmissiometer and a 12 bottle (five liters) rosette. The ship accomplished 77 CTD casts, 77 XCTD and 144 XBTS stations. The ITS Magnaghi and ITS Urania were equipped with WOCE MK-III CTD and each ship accomplished 55 CTD casts during the cruise.

# OGEX1/95 - CTD & XCTD Stations

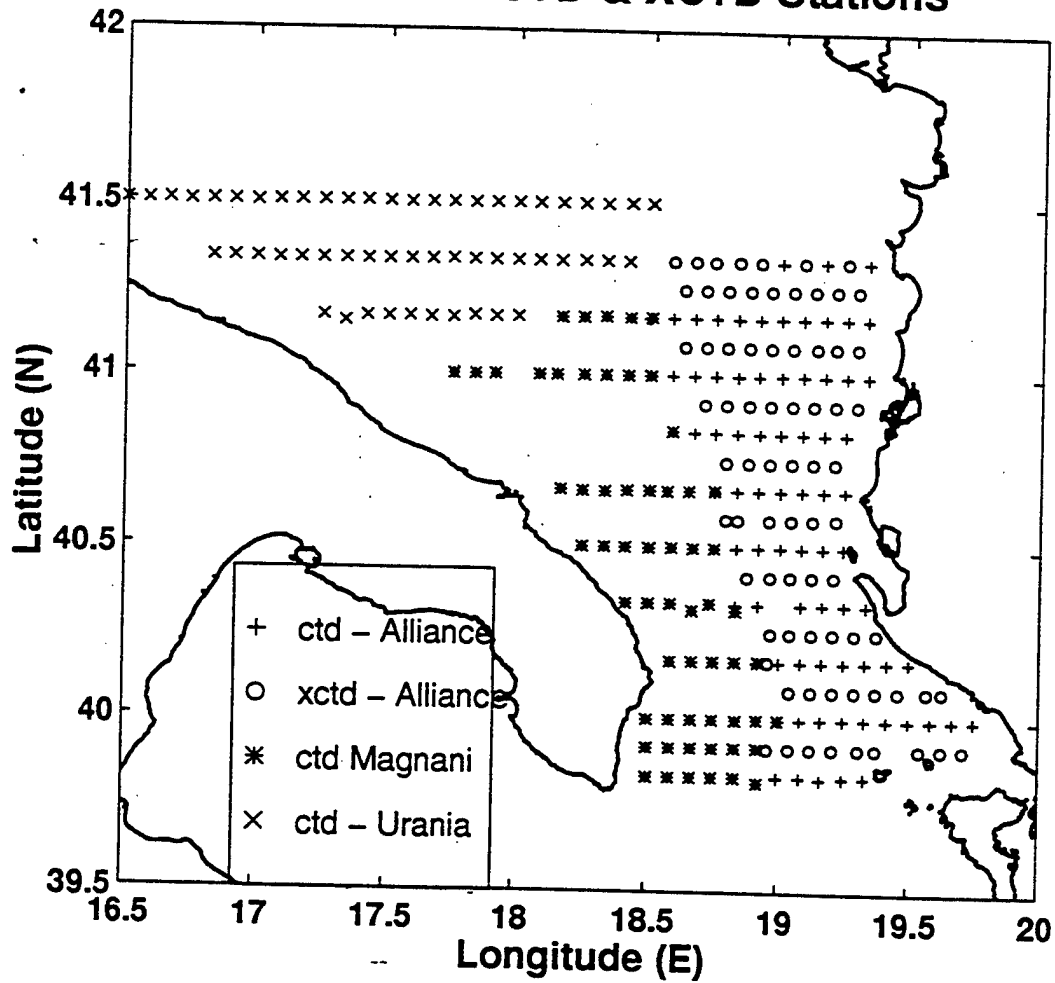


Figure 3: CTD and XCTD sections during the OGEX1 cruise.

### C. MOORING DEPLOYMENTS

A total of ten current meters and ADCP moorings were deployed from NRV Alliance during the cruise. Six moorings (M1-M6) form a two-dimensional sampling array across the Otranto Strait, spanning from Italy to Greece along  $39^{\circ} 50'N$ . They monitored the exchange between the Ionian and Adriatic basins, in particular the inflow of MLIW into the Adriatic. A cross-section of the Otranto Strait with the relative positions and depths of the moored instruments is illustrated in Fig. 4. The other four moorings were deployed in the southern Adriatic. A plan view of the study area shows the locations of the 10 moorings (Fig. 5).

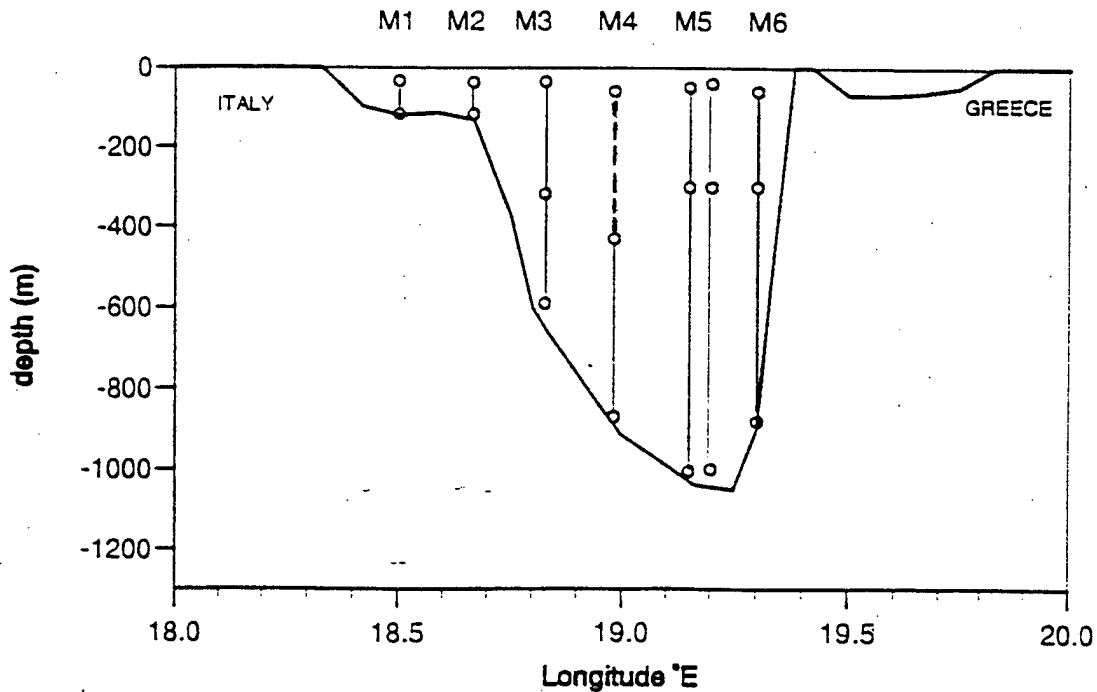


Figure 4: Current meter mooring positions and measurement depths across the Otranto Strait. M4 (middle) is an upward looking moored ADCP.

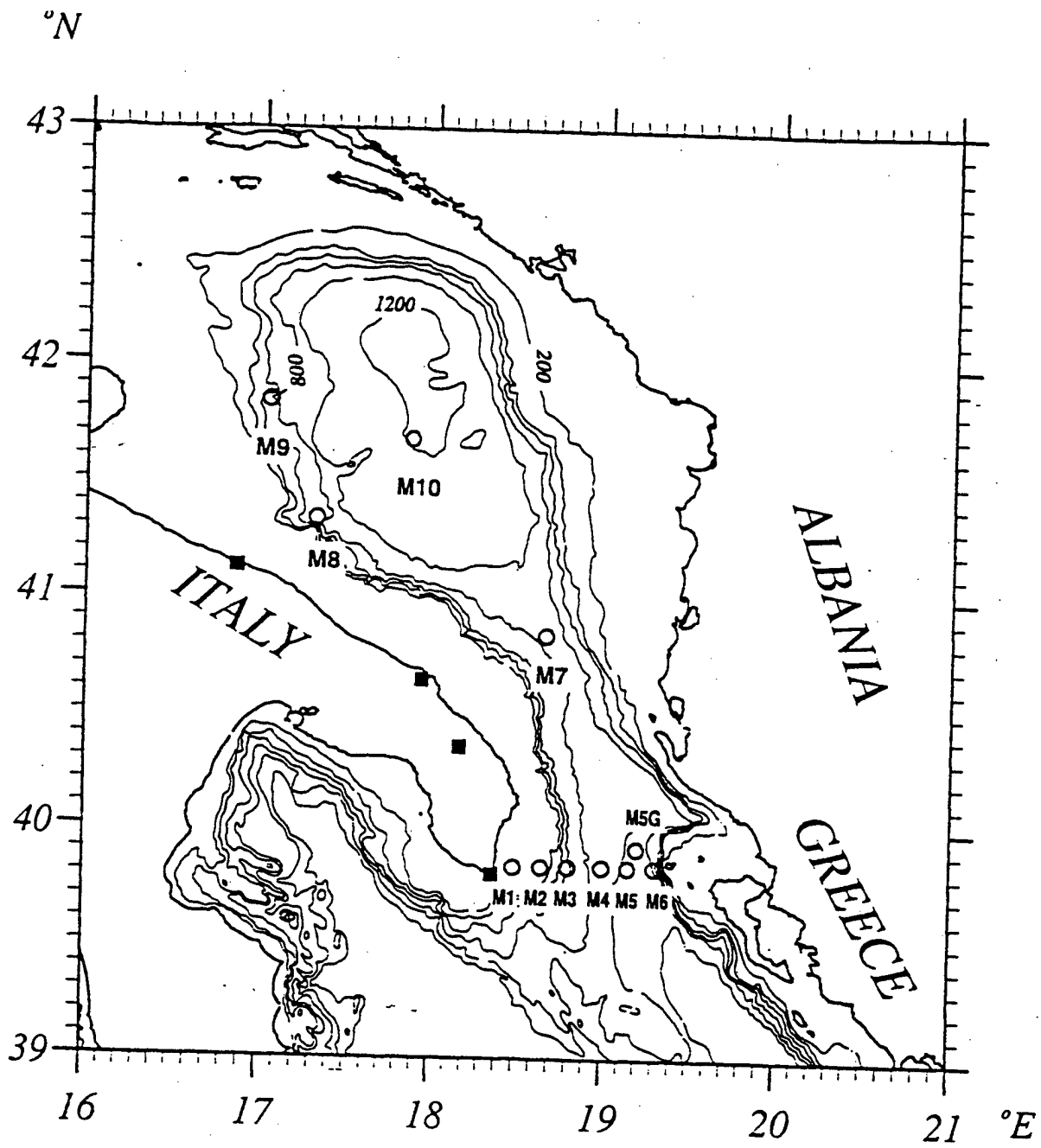


Figure 5: Geographic locations of moorings M1 to M10. Bottom contours in meters.

#### **D. FLOAT AND DRIFTER DEPLOYMENTS**

One ALACE and one MARVOR float were deployed in the Otranto Strait at a nominal depth of 300 m (Poulain and Zanasca, 1998). The main goal of this deployment was to intercompare the capabilities of these devices and prove the concept of tracking intermediate waters with autonomous systems in a regional sea.

Twelve Argos-tracked CODE-type surface drifters were deployed from NRV Alliance and HS Nautilus in the eastern Otranto Strait. Drifter location and sea surface temperature (SST) were obtained through the Argos satellite system (Poulain and Zanasca, 1998).

#### **E. ADCP (ACOUSTIC DOPPLER CURRENT PROFILER)**

Two ADCP systems were used in the cruise. The first one was an upward looking moored ADCP and was located at station M4 in the Otranto Strait (Figs. 4 and 5). The second one was a shipborne ADCP operating on NRV Alliance. The shipborne data were analyzed and studied by (Brauns, 1997). The results will be presented later, along with the moored ADCP data, and will be qualitatively compared with P-vector results.

#### **F. SATELLITE IMAGES**

A new shipboard TERASCAN (Seaspace Corporation) receiver was used onboard the NRV Alliance during the cruise. The system became fully operational on the second half of the cruise. Starting on 22 May, cloud-free images became available and it was possible to see the complex SST patterns in the Otranto Gap. The Advanced Very High Resolution Radiometer (AVHRR) image of 23 May at 17:14Z superimposed with drifter displacements was produced at SACLANTCEN and was made available to us.

#### **G. METEOROLOGICAL DATA**

Meteorological data, especially wind speed and direction, is of extreme importance for the correct interpretation of the observed currents in the Adriatic. They can generate upwelling events and even change the current patterns (Gacic et al., 1996; Poulain, 1998). The parameters measured on board NRV Alliance were air and water temperature, humidity, wind (speed and direction).



#### IV. THE P-VECTOR METHOD

##### A. INTRODUCTION

The P-vector method is a technique to determine absolute geostrophic velocities from hydrographic data. Although it is based on the same dynamical framework of more sophisticated techniques such as the Stommel-Schott(SS) (Stommel and Schott, 1977), Wunsch (Wunsch and Grant, 1978) and Bernoulli (Killworth, 1986) methods, the P-vector method determines the direction first and then determines the magnitude. In previous calculations (Chu, 1995), the method showed reasonable agreement with the expected general circulation of the North Atlantic.

Using the concept of density dependence one can calculate absolute geostrophic currents and use them as initial and boundary conditions for running ocean circulation models, instead of assuming zero velocities at some depth. This will avoid the imbalance between the velocity and density field during the spin-up time (Chu, 1995).

In this thesis the method will be tested in a complex environment, the Adriatic Sea (the Otranto Strait and southern Adriatic), to derive a first approximation the absolute geostrophic currents. The Otranto Strait is known to have a varying reference level from west to east which makes the classical geopotential height approach rather inconclusive (Poulain et al., 1996).

The method is consistent with geostrophy and is assumed to be non-dissipative. The conservation of mass and potential vorticity leads to the condition that the velocity vector is perpendicular to both density ( $\rho$ ) and the potential vorticity ( $q = |f\partial\rho/\partial z|$ ) gradients, and that the velocity can be represented as  $V(x,y,z) = r(x,y,z) * P(x,y,z)$ , where  $P(x,y,z) = (\nabla\rho \times \nabla q) / |\nabla\rho \times \nabla q|$ . The unit vector,  $P$ , is computed from the density field,

and the parameter  $r(x,y,z)$  is determined by the thermal wind relation. Furthermore, an error reduction scheme was also applied in this study (Chu, 1995).

#### B. THERMAL WIND RELATION

The classical thermal-wind equations for calculating geostrophic velocity from density (T and S) profiles are the starting point for the method:

$$u = u_0 + g/f\rho_0 \int \partial\rho/\partial y dz' \text{ (integrated from } z_{\text{ref.}} \text{ to } z \text{ )}, \quad (1 \text{ a})$$

$$v = v_0 + g/f\rho_0 \int \partial\rho/\partial x dz' \text{ (integrated from } z_{\text{ref.}} \text{ to } z \text{ )}, \quad (1 \text{ b})$$

where  $u$  and  $v$  are the two components of geostrophic velocity at a given level ( $z$ ) and  $u_0$ ,  $v_0$  are corresponding values at the reference level ( $z_{\text{ref}}$ ),  $\rho$  is the density,  $\rho_0$  is a typical density value and, finally,  $g$  is the gravitational acceleration.

#### C. CONSERVATION PRINCIPLES

In determining the large scale circulation from hydrographic data we can use, with reasonable correctness, the following assumptions: geostrophic balance, mass conservation and no major isopycnal crossing (Wunsch and Grant, 1982). We can then write:

$$\mathbf{v} \cdot \nabla \rho = 0 \text{ (where } \nabla = i(\partial/\partial x) + j(\partial/\partial y) + k(\partial/\partial z) \text{)}. \quad (2)$$

Differentiating (2) with respect to  $z$  and using the geostrophic and the hydrostatic balance we have:

$$\mathbf{v} \cdot \nabla q = 0, \quad (3)$$

where  $q = f\partial\rho/\partial z$  is the potential vorticity. The use of the approximation  $q = f\partial\rho/\partial z$  can induce a small but systematic error (Neddler, 1985). Equations (2) and (3) above lead to the fact that  $\mathbf{v}$  is perpendicular to both  $\nabla\rho$  and  $\nabla q$  such that  $\mathbf{V} \sim \nabla\rho \times \nabla q$  (Chu, 1995), if

$$|\nabla\rho \times \nabla q| \text{ is } \neq 0. \quad (4)$$

Killworth (1986) emphasized the importance of using the  $\rho$ - $q$  space rather than the T-S space for determining the absolute velocities.

#### D. THE P-VECTOR FIELD

Under the condition specified by (4) the unit vector  $\mathbf{P}$  (Fig. 6) will exist and will lie on the intersection of the potential density and potential vorticity surfaces:

$$\mathbf{V} = r(x, y, z)\mathbf{P}. \quad (5)$$

Applying the thermal wind relation to any of two different depths  $z_i$  and  $z_j$  a set of algebraic equations for determining the parameter  $r$  is obtained:

$$r^{(i)}P_x^{(i)} - r^{(j)}P_x^{(j)} = \Delta u_{ij}, \quad (6)$$

$$r^{(i)}P_y^{(i)} - r^{(j)}P_y^{(j)} = \Delta v_{ij}. \quad (7)$$

These are linear algebraic equations for  $r^{(i)}$  and  $r^{(j)}$ , where  $r^{(i)}$  is in fact  $r^{(i)} = r(x, y, z_i)$  and

$$\Delta u_{ij} = g/f\rho_0 \int \partial\rho/\partial y dz' \text{ (integrated from } z_i \text{ to } z_j), \quad (8)$$

$$\Delta v_{ij} = g/f\rho_0 \int \partial\rho/\partial x dz' \quad (\text{integrated from } z_i \text{ to } z_j), \quad (9)$$

The trapezoidal rule can be used to integrate (8) and (9). The parameter  $r$  can be determined, and hence the absolute geostrophic velocities can be obtained.

If

$$\begin{vmatrix} P_x^{(i)} & P_x^{(j)} \\ P_y^{(i)} & P_y^{(j)} \end{vmatrix} \neq 0,$$

the algebraic equations (6) and (7) have definite solutions for  $r^{(i)}$  ( $i \neq j$ ):

$$r^{(i)} = \frac{\begin{vmatrix} \Delta u_{ij} & P_x^{(i)} \\ \Delta v_{ij} & P_y^{(i)} \end{vmatrix}}{\begin{vmatrix} P_x^{(i)} & P_x^{(j)} \\ P_y^{(i)} & P_y^{(j)} \end{vmatrix}}.$$

With the value of  $r$  we can then calculate the absolute velocity.

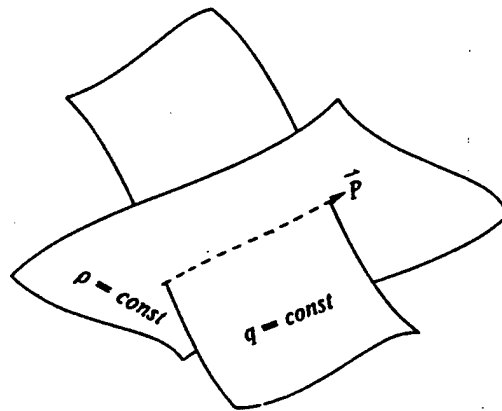


Figure 6: The intersection between  $\nabla\rho$  and  $\nabla q$ , forming the P-vector (from Chu, 1995).

### E. SOURCES OF ERROR

For a given level,  $z = z_i$ , there are (N-1) sets of equations for computing  $r^{(i)}$ , where N is the total number of levels in the density field. Under normal conditions the thermal wind equations should provide the same solution. However, due to instrumentation errors and to truncation errors, the parameter  $r^{(i)}$  may vary with i.

### F. THE MAXIMUM TURNING ANGLE PRINCIPLE

If we define a turning angle ( $\alpha$ ) as the angle between the x axis and the P-vector and take any two pair of levels z, we can say that:

$$P_x = \cos \alpha \quad \text{and} \quad P_y = \sin \alpha. \quad (10)$$

The determinant  $\begin{vmatrix} P_x^{(i)} & P_x^{(j)} \\ P_y^{(i)} & P_y^{(j)} \end{vmatrix}$  will be equal to  $\sin \alpha_{ij}$  where,

$\alpha_{ij} = \alpha^{(i)} - \alpha^{(j)}$  indicates the  $\beta$  spiral turning between the pair of two z levels. In the case of the Beta-Spiral method (Stommel-Schott, 1977) if  $\alpha_{ij}$  is close to zero, the method fails to determine the corresponding absolute velocity. Chu (1996) notes that the  $\beta$ -spiral method differs from the P-vector method in that the later has (N-1) choices (degrees of freedom) for picking up a level ( $z_i$ ) for the computation. This means that we have freedom to ignore those levels leading to very small turning angles. To assure the best solution, we adopt a maximum turning angle principle to obtain the level  $z_{ij}$  :

$$|\sin(\alpha_{ij})| = \text{Max} |\sin(\alpha_{ij})| \quad \text{for} \quad (i \neq j).$$

### G. ERROR REDUCTION SCHEME

Due to instrumentation and truncations errors, the computed velocity field contains computational noise. To eliminate this noise an iteration procedure is used, as long as the errors can lead to a non-conservative field either for mass or for potential vorticity (Chu, 1995). Using the superscript (L) to denote iteration steps and defining the residues (R) of each solution we can say that:

$$R_p^{(L)} = \cos \alpha_p^{(L)} = |\mathbf{V}^{(L)} \cdot \nabla \rho| / |\mathbf{V}^{(L)}| |\nabla \rho| \text{ and}$$

$$R_q^{(L)} = \cos \alpha_q^{(L)} = |\mathbf{V}^{(L)} \cdot \nabla q| / |\mathbf{V}^{(L)}| |\nabla q|,$$

where  $\alpha_p^{(L)}$  is the angle between  $\mathbf{V}^{(L)}$  and  $\nabla \rho$ ,  $\alpha_q^{(L)}$  is the angle between  $\mathbf{V}^{(L)}$  and  $\nabla q$ , and  $R_p^{(L)}$  and  $R_q^{(L)}$  are the scale residues of the density and potential vorticity conservation equations at each point for the  $L^{\text{th}}$  field iteration. Defining LCI as the accuracy of the solution at a given point (x,y,z) and GCI as the overall accuracy of the solutions, we can then set up the iteration scheme such that we proceed in further steps until  $\mathbf{V}^{(L+1)}$  is more accurate than  $\mathbf{V}^{(L)}$ . This will happen when  $\text{GCI}^{(L+1)} \geq \text{GCI}^{(L)}$  (Fig. 8).

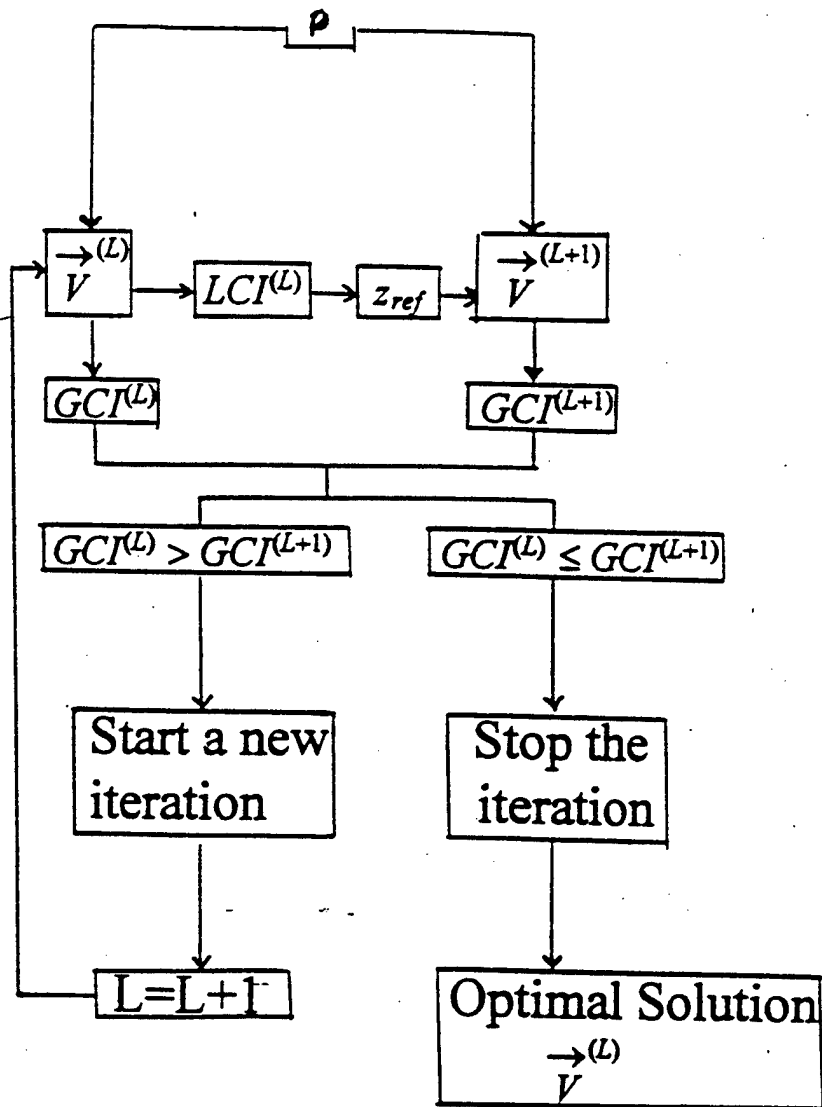


Figure 7: The P-vector iteration scheme (from Chu, 1995).



## V. RESULTS

This Chapter presents the results of the hydrographic data analyses, in the form of T-S diagrams, vertical and horizontal sections of temperature, salinity and sigma-t. Plots of relative and absolute (obtained by the P-vector method) geostrophic circulations are presented. Wind, current meter and drifter data collected during the OGEX1 cruise are displayed. Some discussions of the individual results are provided.

The first procedure in the analysis process was to create a regular grid using the data collected as shown in Fig. 3. This was necessary to contour the data and to match the DBDB5 topography. The latter was used to force the P-vector method to cease its calculations upon encountering the bottom. The new grid has 22 north-south increments (from 39° 45'N to 41° 30'N) and 43 east-west increments (from 16° 30'E to 20° 00'E) and a grid spacing of 5 minutes, similar to the one used between actual stations. In the vertical, the hydrographic data were averaged over 10 m ( $\pm$  5 m) around levels separated by 20 m. Hence for the P-vector calculations there are 54 horizontal sections, separated by 20 m and 21 cross-sections located at every mid point between pairs of the 22 latitudes.

### A. HYDROGRAPHIC DATA ANALYSES

As stated previously, the major water masses present in the southern Adriatic are Adriatic Deep Water (ADW) and Modified Intermediate Levantine Water (MLIW). In addition there are two surface waters: Adriatic Surface Water (ASW) and Ionian Surface Water (ISW). The T-S diagrams in Figs. 8 and 9 show the locations of these water masses in the T-S space.

The MLIW is identified in only three diagrams (it is not present in the ITS Urania diagram). This is the saltiest water found in the Adriatic ( $>$  38.7 psu) and it is relatively warm ( $>$

14.7 °C) (Artegiani et al., 1993). It is easily identified by the arrowhead shape at the right on the T-S diagram for NRV Alliance (Fig.8) and ITS Magnaghi (Fig. 9a). It is also clearly seen in the Otranto Strait cross-section (Fig. 10) as a core at about 180 m depth east of approximately 19.1°E, which is consistent with the historical core depth for MLIW of 200 m (Orlic et al., 1992). The horizontal spatial extent of MLIW at 200 m (Fig. 11), shows that it can be traced as far north as 41.5 °N, along the Albanian coast. In the vertical cross-section (Fig. 10 - middle panel), it is also evident on the eastern flank of the Otranto Strait.

ADW is present in all diagrams. It appears to result from mixing of NAW and MLIW (Orlic et al., 1992). It occupies most of the volume at the Otranto Strait cross-section (Fig. 10, sigma-t in bottom panel). It is depicted by the yellow-greenish color below approximately 350 m depth.

Both the ASW and ISW are identified in the left and right (upper) portions, respectively, of the T-S diagrams (Figs. 8 and 9) and in the 40 m depth horizontal maps (Fig. 12). The ISW flows into the Adriatic on the western flank of the Otranto Strait (Fig. 10) and along the Albania coast (Fig. 12, top panel). In contrast, the ASW is seen as a very low salinity surface tongue outflowing on the Italian shelf (see Figs. 10 and 12).

The OGEX1 cruise plan was designed in such way that the eastern portion was surveyed by NRV Alliance, and the western portion by ITS Magnaghi and ITS Urania (Fig. 3). This east-west partitioning can be seen in the T-S diagram for each ship (Figs. 8 and 9), and in the horizontal and vertical sections (Figs. 10 to 11). The NRV Alliance survey demonstrates warmer and more saline waters than both the ITS Urania and ITS Magnaghi surveys. This again confirms the inflow of Ionian water along the eastern portion of the basin. A tendency to extend farther north would be expected, due the cyclonic circulation, typical of the southern Adriatic (Buljan and Zore-Armanda., 1976), although such

spreading was not sampled during the OGEX1 cruise. Instead, a relatively warm and low salinity water mass originating from the runoff of the Albanian rivers can be seen on the Albanian shelf in Fig. 12. It corresponds to the minimum densities observed during the OGEX1 cruise.

### TS Diagram & Sigma-T contours

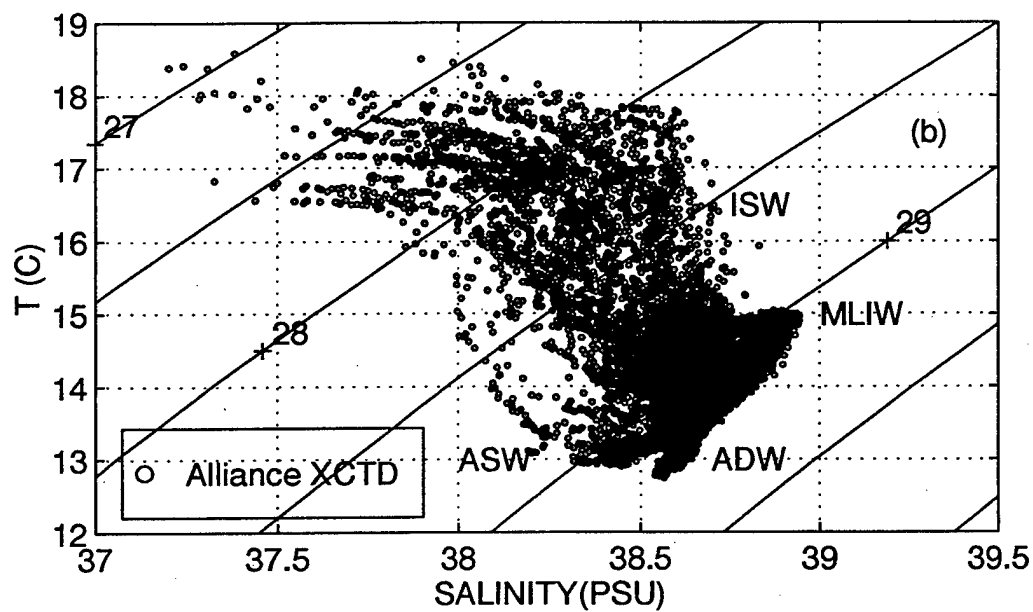
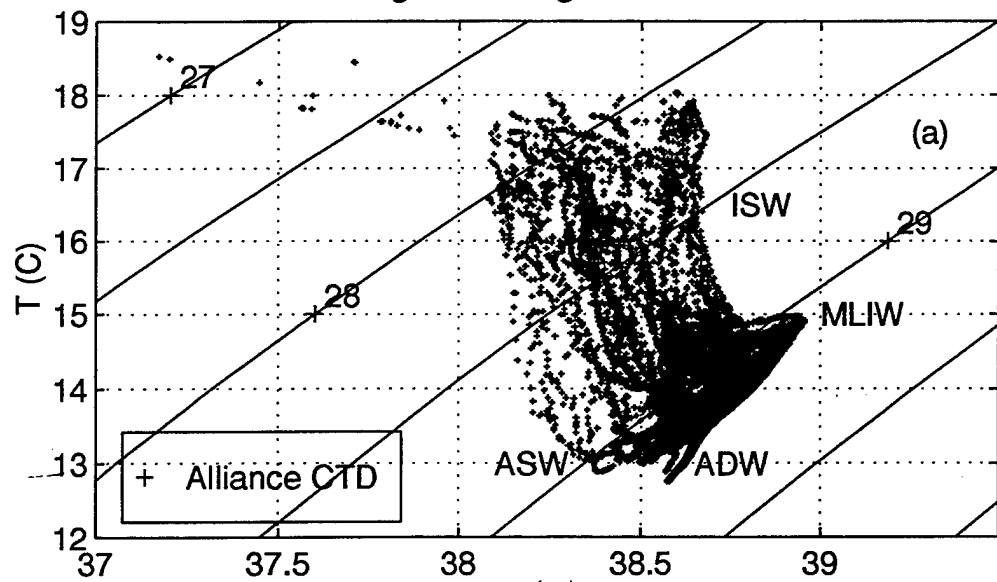


Figure 8: T-S diagram and sigma-t contours from the NRV Alliance data set. CTD (a) and XCTD (b).

### TS Diagram & Sigma-T Contours

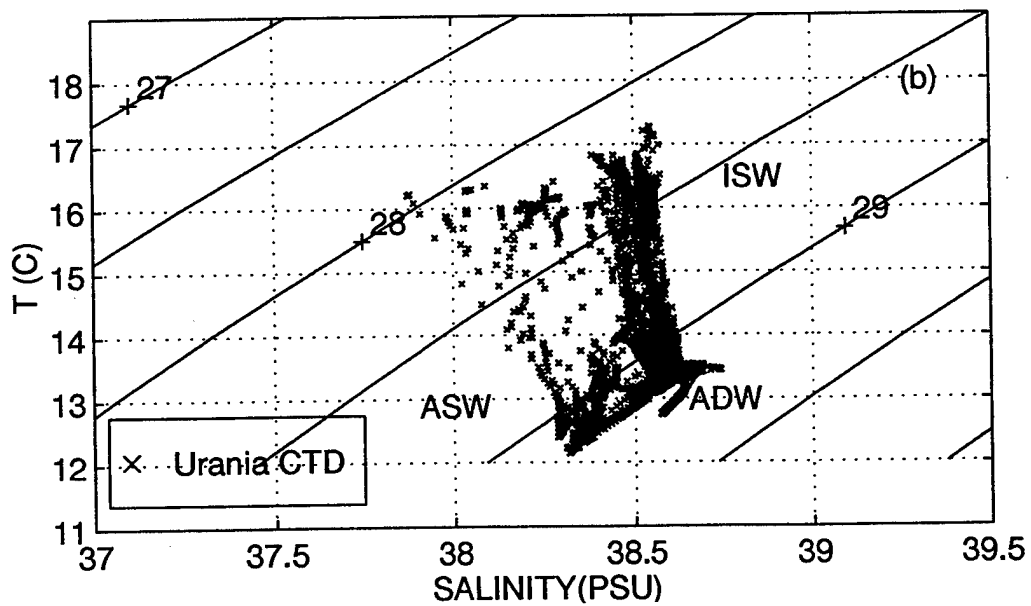
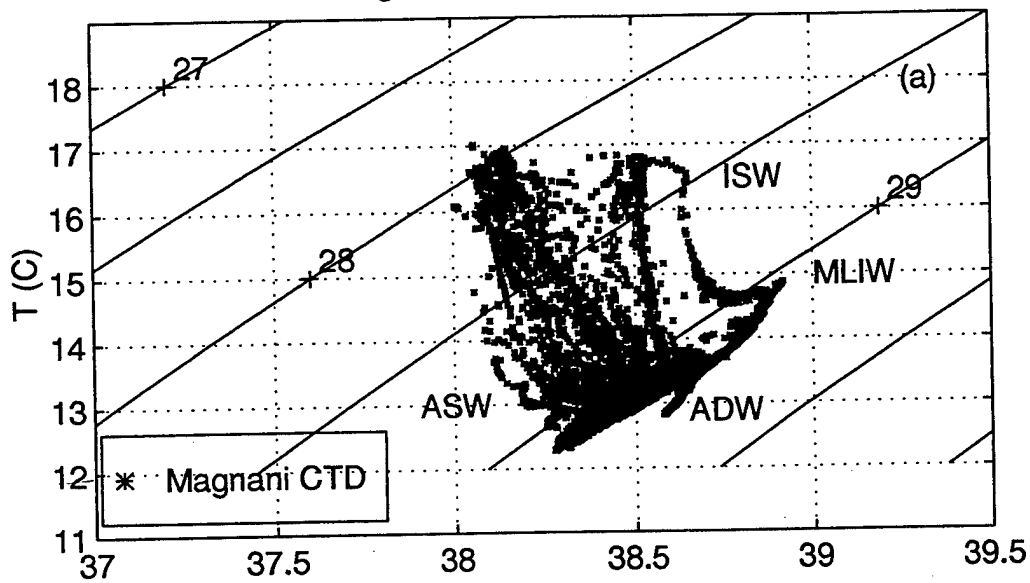


Figure 9: Same as Fig. 8 but for ITS Magnaghi CTD (a) and ITS Urania CTD (b).

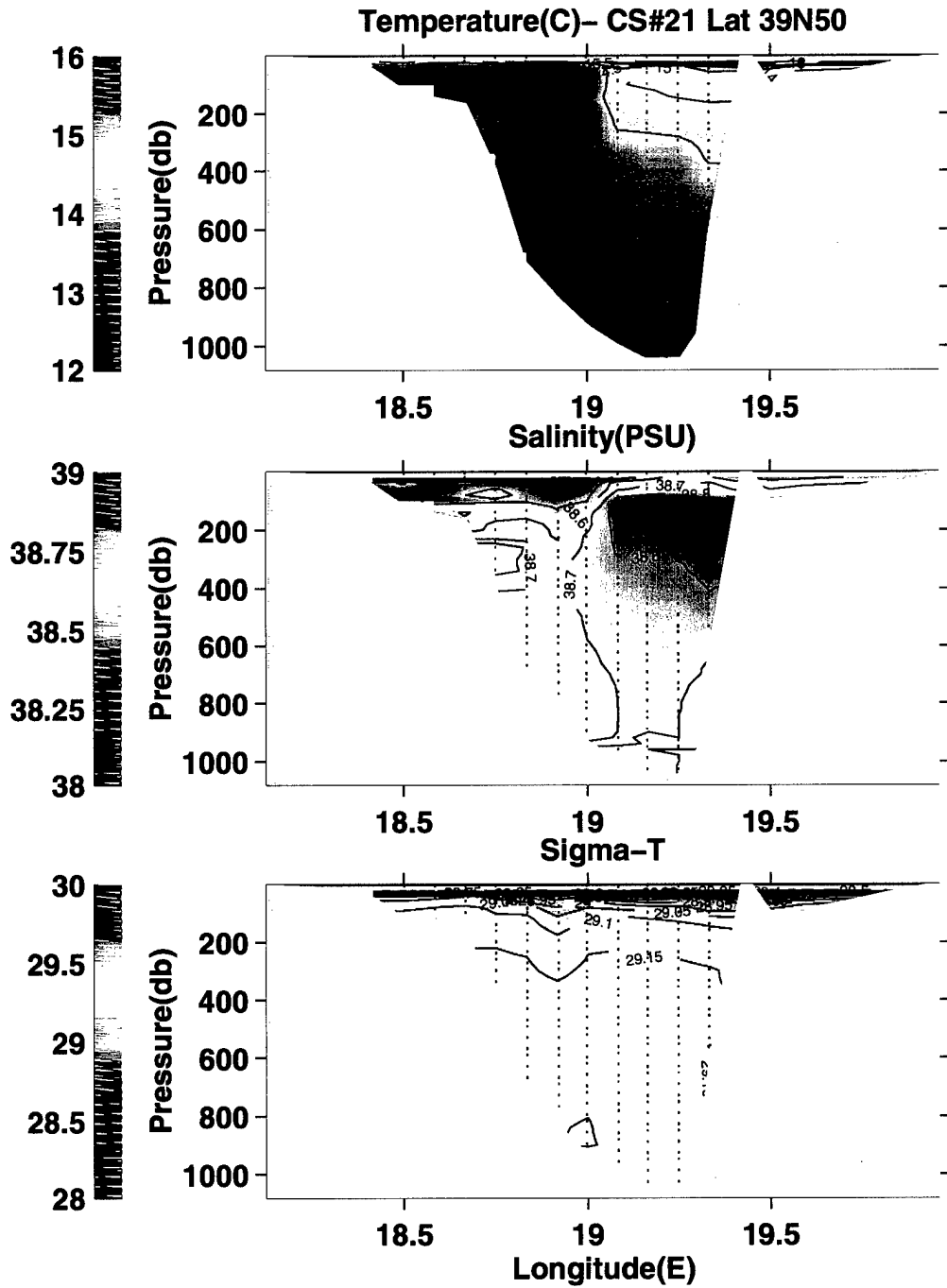


Figure 10: Temperature ( $^{\circ}\text{C}$ ), salinity (PSU) and sigma-t for cross-section 21 ( $39^{\circ} 50' \text{N}$ ) across the Otranto Strait.

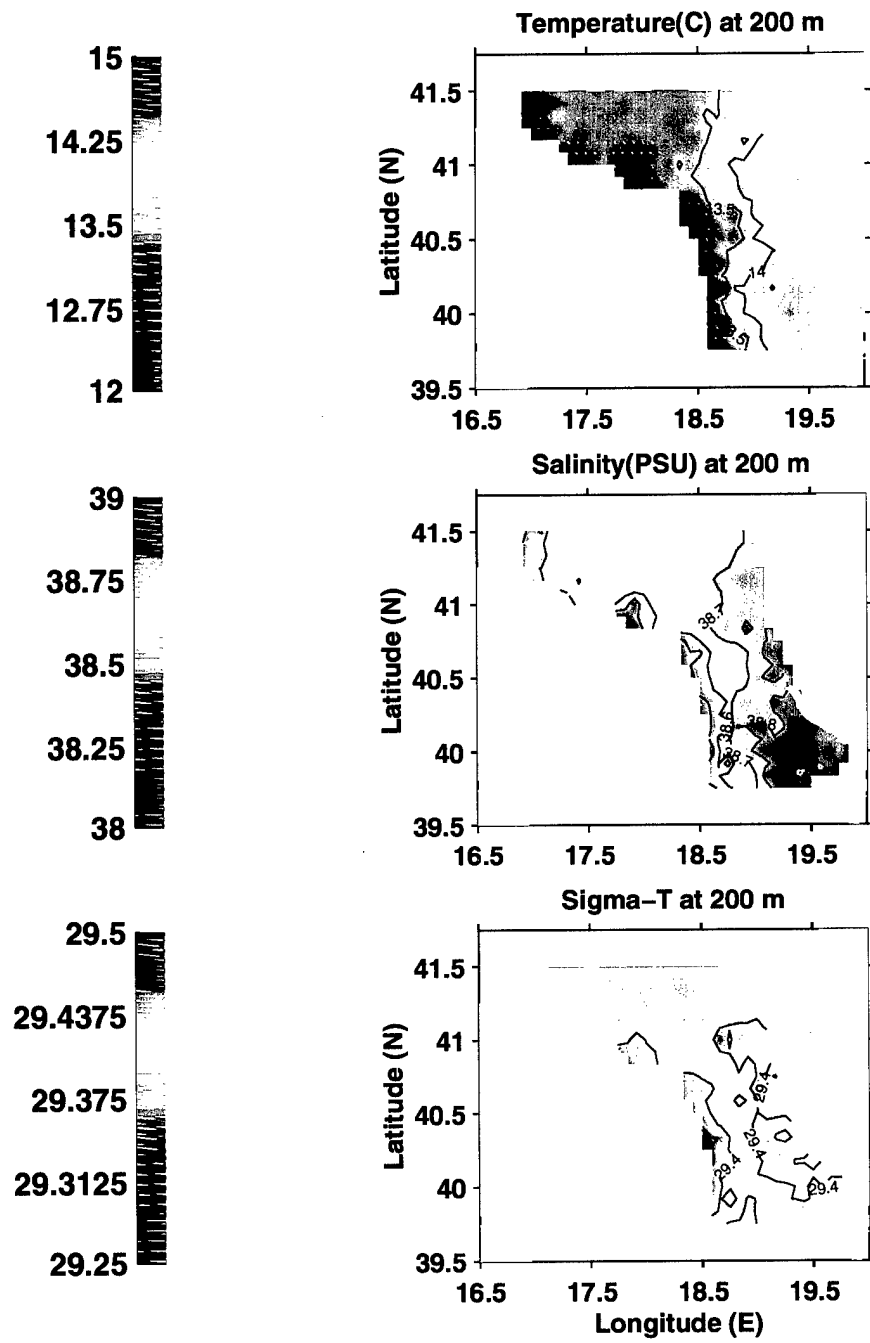


Figure 11: Temperature ( $^{\circ}\text{C}$ ), salinity (PSU) and sigma-t contours at 200 m depth.

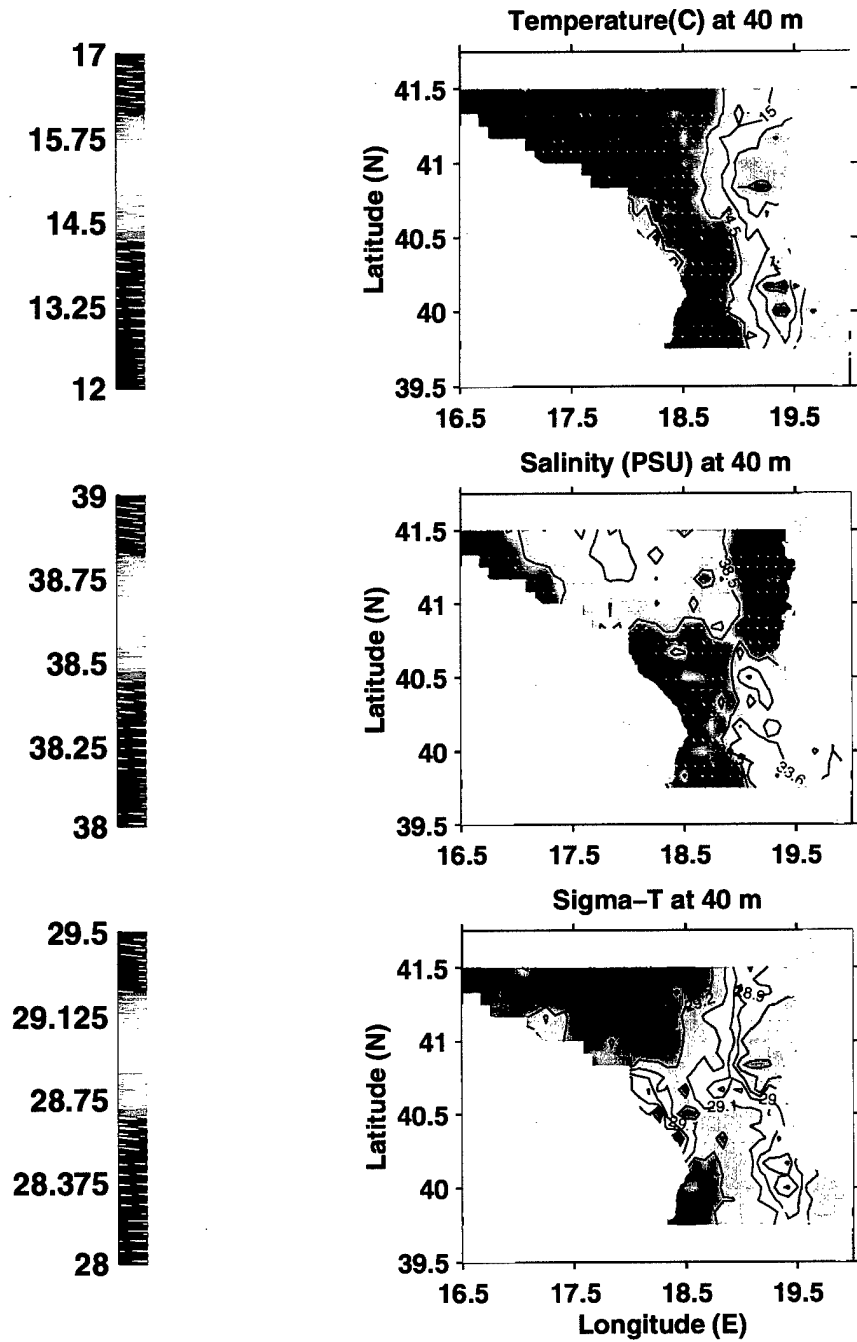


Figure 12: Same as Fig. 11 but at 40 m depth.

## C. GEOSTROPHIC CIRCULATION MAPS

### 1. Relative Geostrophic Maps

The hydrographic data were interpolated onto a uniform horizontal array with 5 minute grid size (roughly 10 km). Relative geostrophic flows were calculated using the classical thermal wind equations (1a and 1b). The results are presented as horizontal vector plots in Figs. 13, 14 and 15. The near surface circulation (40 m) with respect to the flow at 200 m (Fig. 13), shows clearly the inflow of the ISW in the eastern Otranto Strait and the southern limb of the cyclonic gyre circulation around the South Adriatic Pit, with a maximum speeds approaching 15 cm/s. The geostrophic shear between 200 m and 800 m (Fig. 14) discloses very small meridional currents in the Otranto Strait and a reduced signature of the cyclonic gyre around the South Adriatic Pit. Most of the velocity shear in the water column can be represented by considering the geostrophic flow at 40 m with respect to 800 m (Fig. 15). The situation is similar to that of Fig. 14. All three geostrophic maps reveal the presence of a strong anticyclone near  $41^{\circ}\text{N}$  and  $18.67^{\circ}\text{E}$  where the geostrophic shear can as large as 40 cm/s. This mesoscale feature will be discussed in the next Chapter. Counter currents are also seen near the southern Albanian coast with flow in the south and southeast directions.

### 2. P-vector Sections

The absolute geostrophic velocity, as calculated by the P-vector method, at the depths of 40 and 200 m are shown in Figs. 16 and 17, respectively. The 40 m depth map confirms rather well the cyclonic geostrophic circulation in the southern Adriatic mainly north of  $41^{\circ}\text{N}$ . At the Otranto Strait the flow is relatively weak with an inflow present both east and west of  $19^{\circ}\text{E}$  while an outflow vein is evident in the center. The maximum absolute geostrophic speed is approximately 10-12 cm/s.

The flow at 200 m depth is even weaker. Again the cyclonic gyre north of  $41^{\circ}$  N is recognized, although it seems to be embedded in small mesoscale circulation patterns. At the strait the flow mimics the pattern at 40 m, but with much smaller magnitudes (1-3 cm/s). An anticyclone feature is seen at the 40 m level near  $41^{\circ}$ N and  $18.67^{\circ}$ E with speeds reaching 15 cm/s. The P-vector results indicate that such feature is trapped in the surface layers as the flow becomes slightly cyclonic at 200 m (Fig. 17). Strong southward currents are evident along the Albanian slope near  $40.5^{\circ}$ N and  $19^{\circ}$ E.

geostrophic velocity level: 2 ref\_level = 200(m)

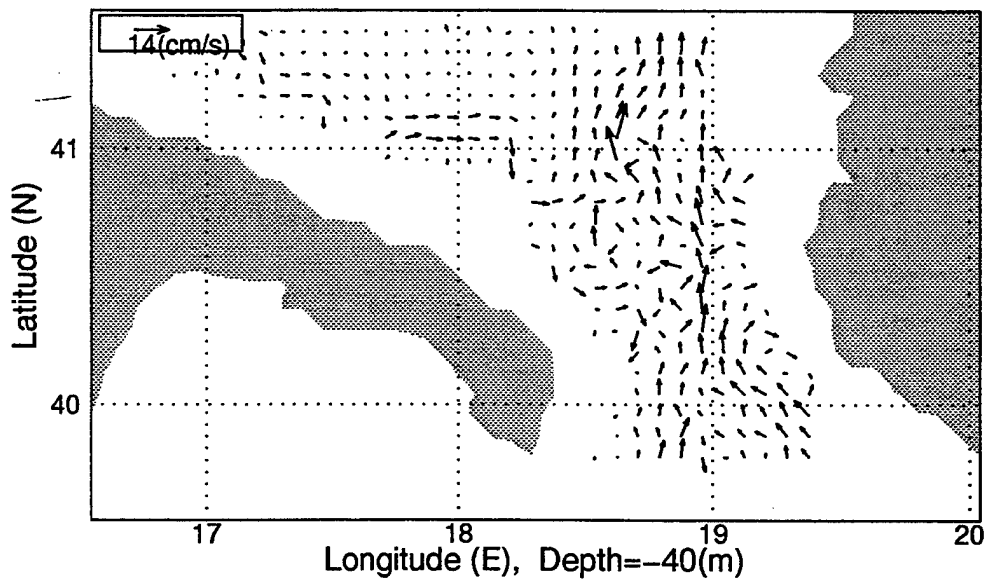


Figure 13: Geostrophic velocity at 40 m relative to 200 m.

geostrophic velocity level: 10 ref\_level = 800(m)

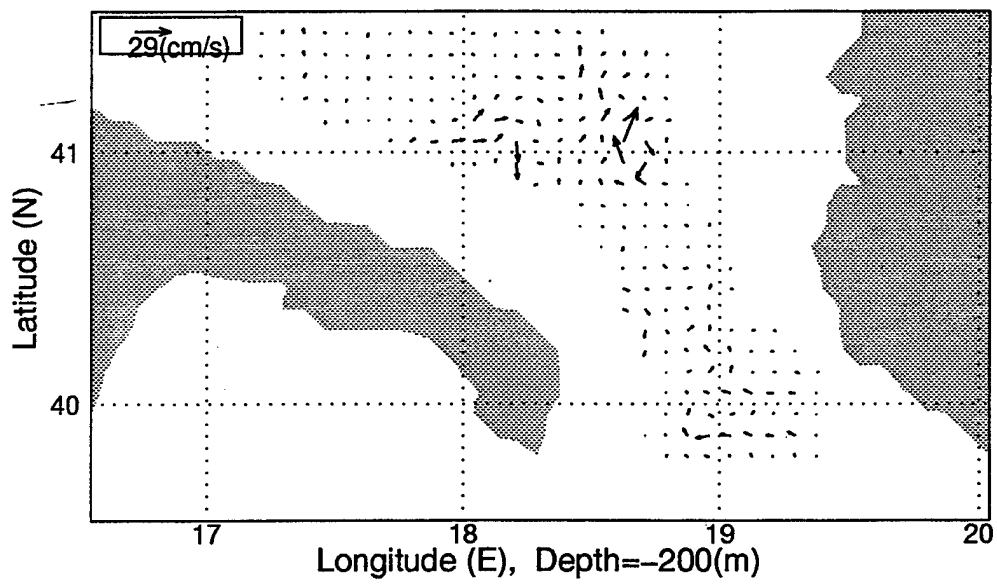


Figure 14: Geostrophic velocity at 200 m relative to 800 m.

geostrophic velocity level: 2 ref\_level = 800(m)

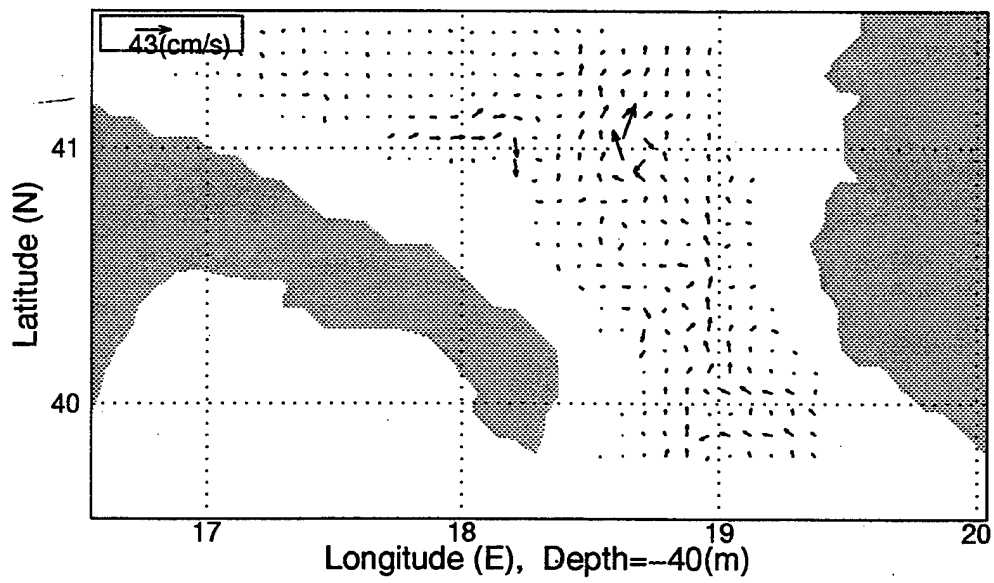


Figure 15: Geostrophic velocity at 40 m relative to 800 m.

P-vector Absolute Geostrophic Velocity

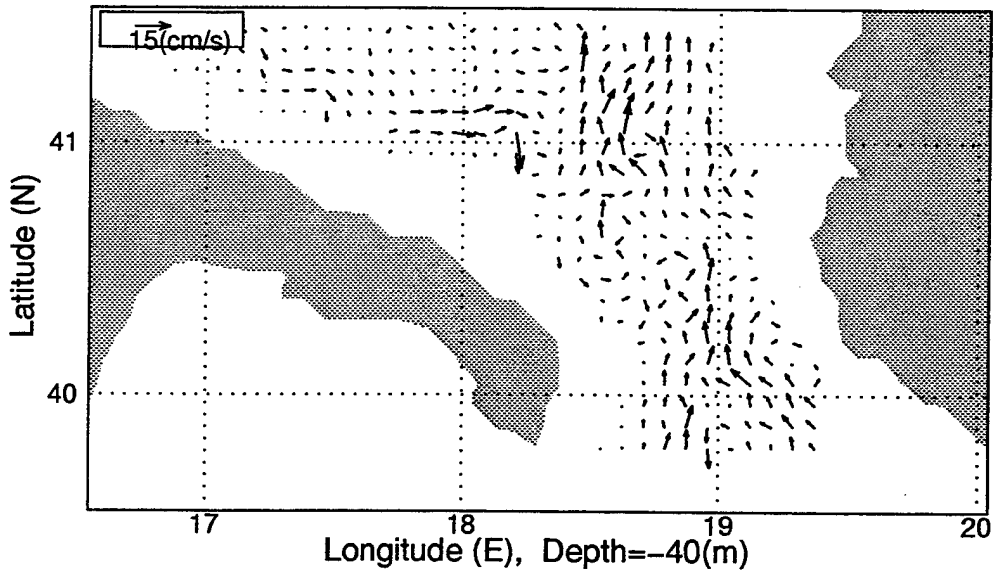


Figure 16: P-vector absolute geostrophic velocity at 40 m.

P-vector Absolute Geostrophic Velocity

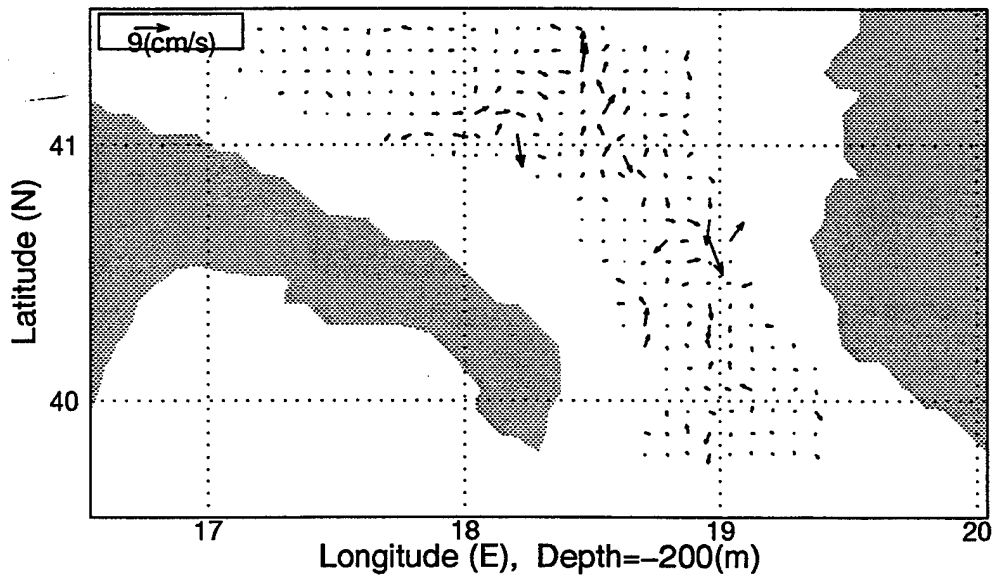


Figure 17: Same as Fig. 16 but at 200 m.

In order to compare with the moored current meter data, cross-sections of the north-south absolute geostrophic flow as determined by the P-vector method are presented. They correspond to the deployment latitudes of moorings M1-M6 ( $39^{\circ} 50'N$ ); M7 ( $40^{\circ} 49'N$ ) and M8 ( $41^{\circ} 20'N$ ).

The cross-section at  $39^{\circ} 51'N$ , in the Otranto Strait (Fig. 18), depicts two inflowing (from the Ionian Sea into the Adriatic Sea) surface current patterns, one to the west of approximately  $18.9^{\circ} E$  and the other east of approximately  $19.1^{\circ}E$ . Between both inflows a weak outflow is observed. In general the flow is significant above 300 m. Below that level the P-vector calculations show negligible absolute geostrophic velocities.

The cross-section at M7 is depicted in Fig. 19. It shows a series of north and south filaments between  $17^{\circ} 30'E$  and  $19^{\circ} E$ . The most significant magnitudes are approximately between  $18.5^{\circ}$  and  $18.6^{\circ} E$ . The maximum speed is 10-12 cm/s. Mid-depth speeds are about twice that observed in the Strait.

The last cross-section, at the same latitude of mooring M8, (Fig. 20) exhibits a pattern similar to the one at M7. The most noteworthy feature is the large (4-6 cm/s) northward flow approximately between  $18.3^{\circ}E$  and  $18.5^{\circ} E$ . These currents are associated with the high baroclinic shear created by the fresh water riverine input from Albania. This river runoff is depicted in Fig. 12, as a relatively warm (top panel) and fresh water (middle panel) east of approximately  $19^{\circ}E$  and north  $40.5^{\circ}N$ .

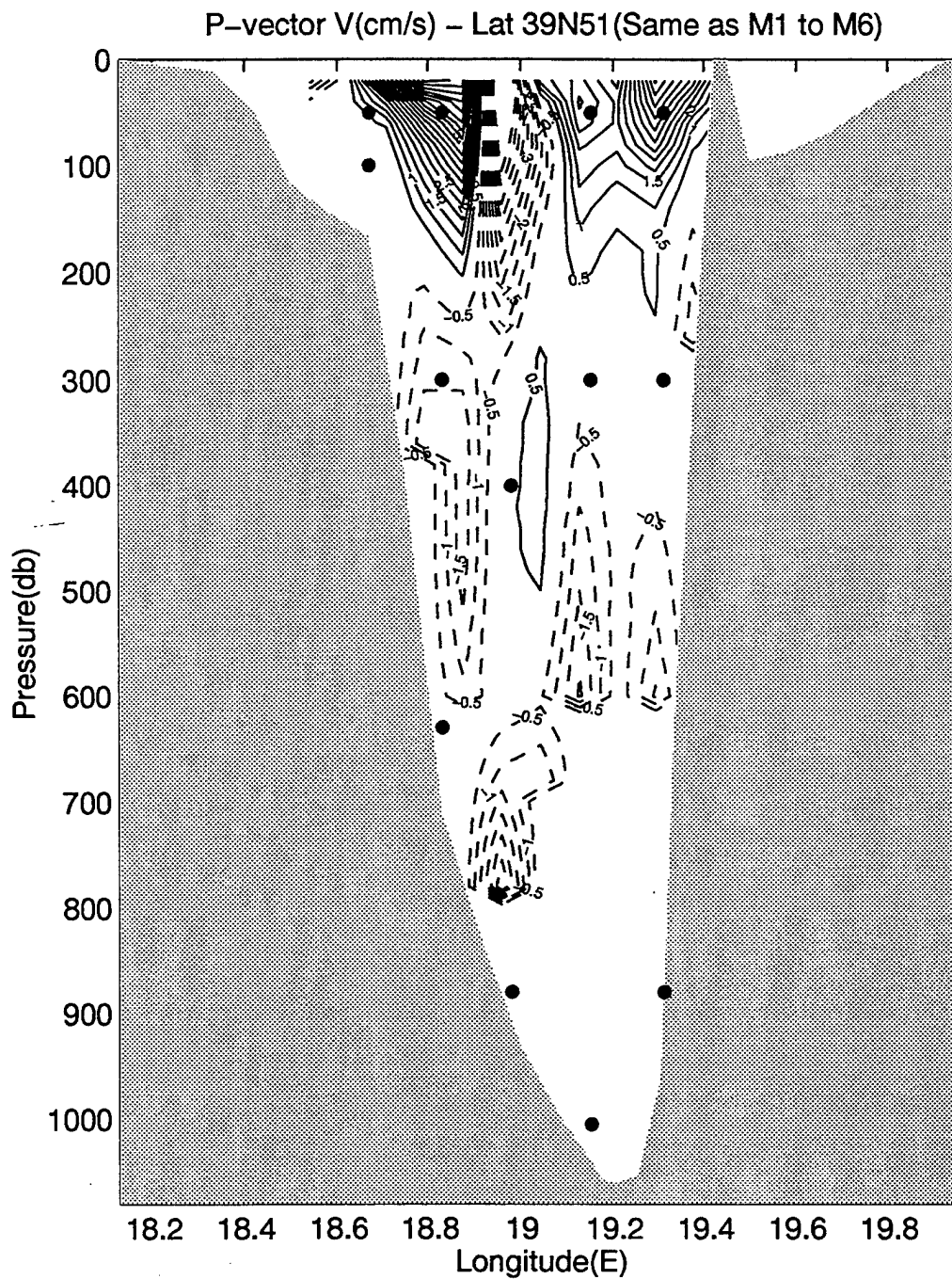


Figure 18: P-vector v-component (cm/s). Cross-section at latitude  $39.75^{\circ}$  N (same as Mooring M1 to M6). Solid (dashed) lines represent northward (southward) flows. Solid dot symbols represent the locations of the moored current meters.

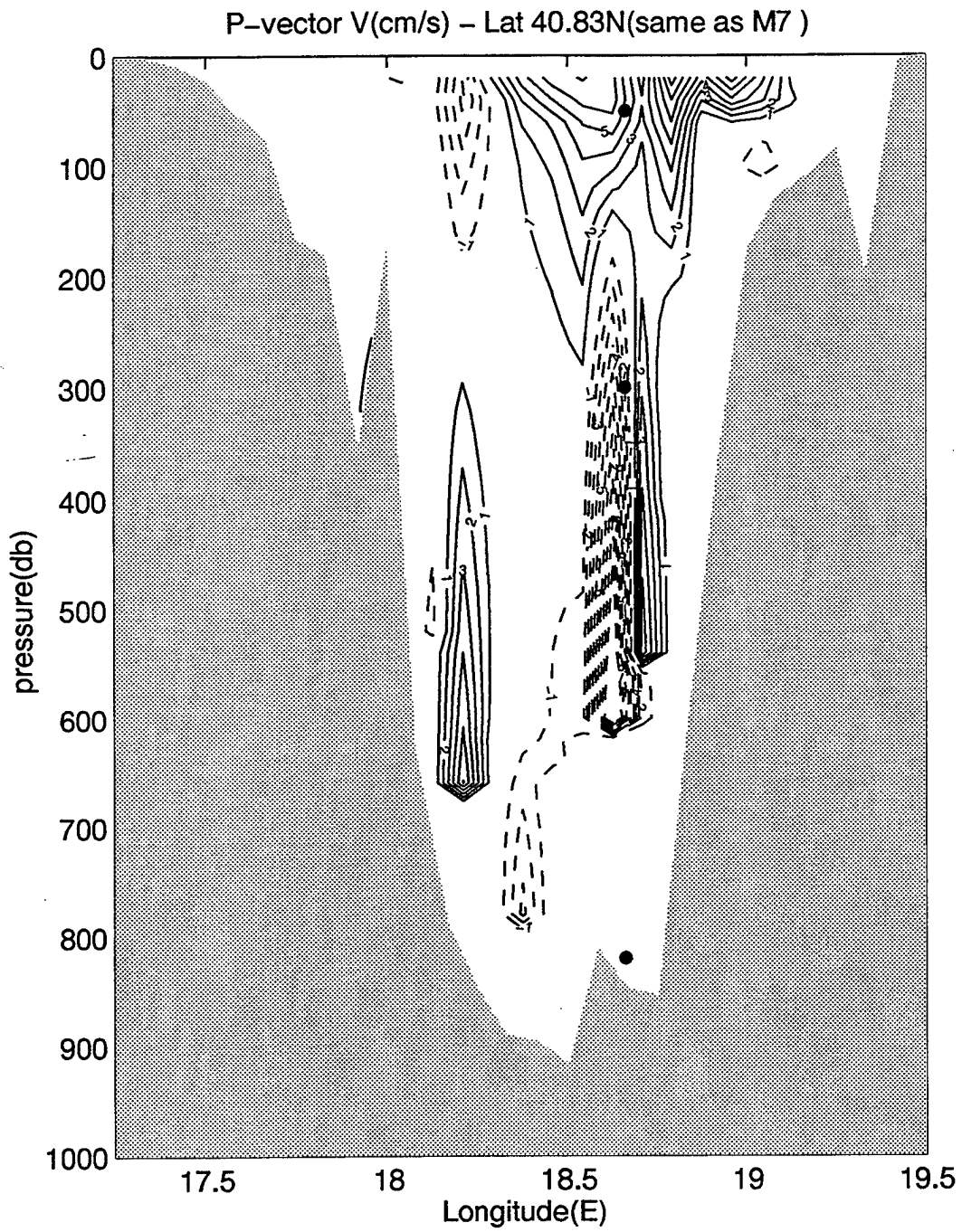


Figure 19: Same as Figure 15 but for latitude  $40.83^{\circ}$  N (same as Mooring M7).

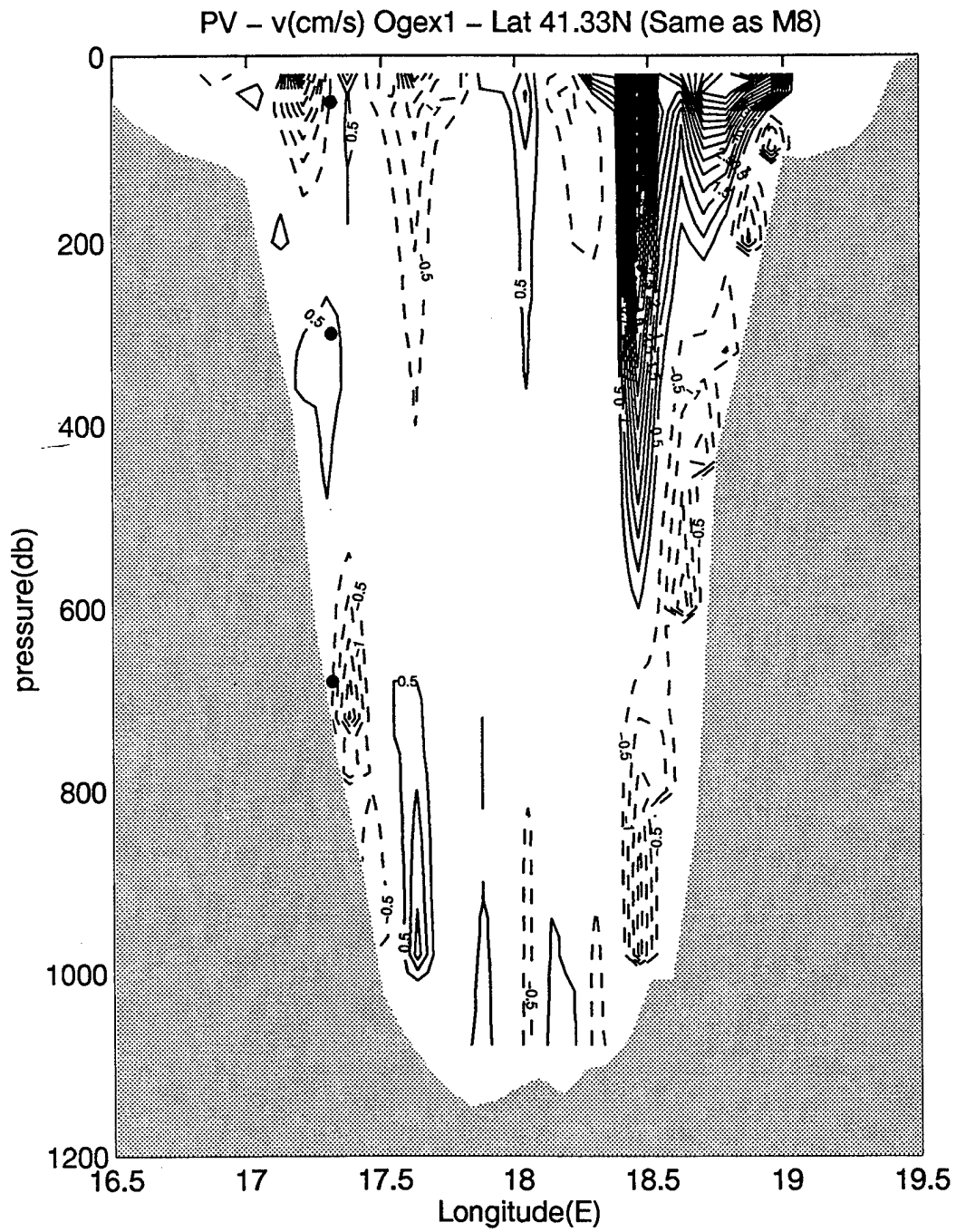


Figure 20: Same as Figure 15 but for latitude  $41.33^{\circ}$  N (same as Mooring M8).

## C. MOORED CURRENT METER AND DRIFTER DATA

### 1. Moored Current Meter Data Time Series

The processed moored current meter data consist of the actual raw measurements and the low pass filtered north-south (v) and east-west (u) components. The so-called 24m214 low pass digital filter was used to remove tidal/inertial variations from the original time series (Thompson, 1983).

In order to obtain a general feeling for the evolution of the current meter data, time series of the north-south velocities during the cruise period were analyzed. The most noteworthy time series (M3 and M6) are presented in Figs. 21 and 22. The latter (M6) is presented along with the north component of the wind speed during the same time period. The M6 current meter time series, at the surface and at 300 m, show the influence of the wind remarkably well. The wind reverses from north to south in the morning of May 21 and the currents at 50 m and at 300 m respond to this reversal by weakening and eventually reversing (flowing southward) approximately one day later (Fig. 21 a and b). The opposite occurs at mooring M3 (Fig. 22 a and b). This mooring is located on the western flank of the Otranto Strait (Fig. 3). While at M6 the water is reversing from northward to southward (both at the surface and at 300 m), at M3 the situation is opposite and the currents change from southward to northward. This opposite behavior at M3 might correspond to compensating inflow/outflow currents on the western side. No wind data is available in western Otranto Strait to explore this speculative conclusion. The current meter data will be used later to estimate the current meter accelerations and assess the geostrophic balance of the flow.

Northward Component (v) of Wind (NRV Alliance) and Currents (Mooring M6)

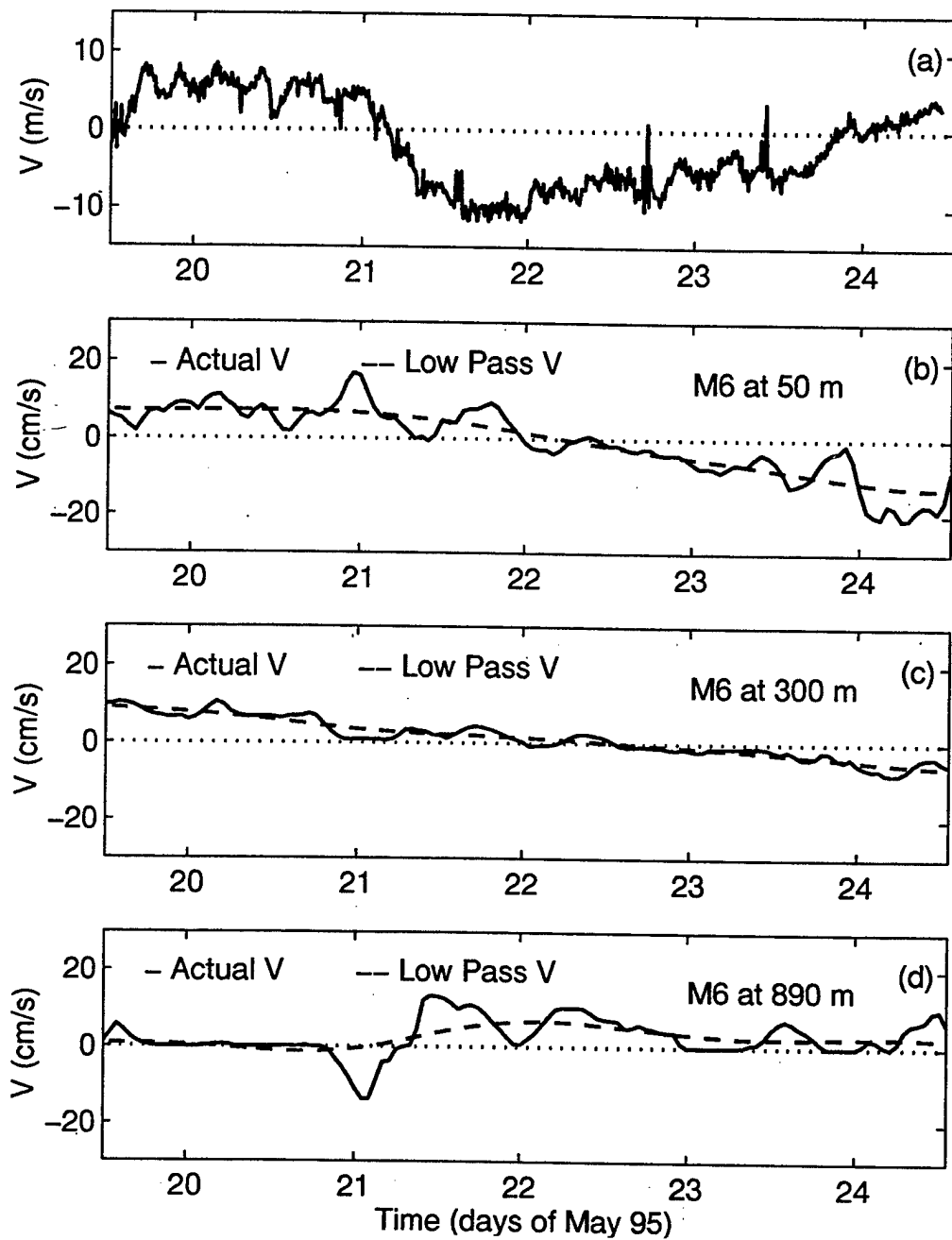


Figure 21: North-south components of the wind velocity (a) and of the raw (actual) and low pass filtered currents at mooring M6 for three depths, 50 m (b), 300 m (c) and 890 m (d).

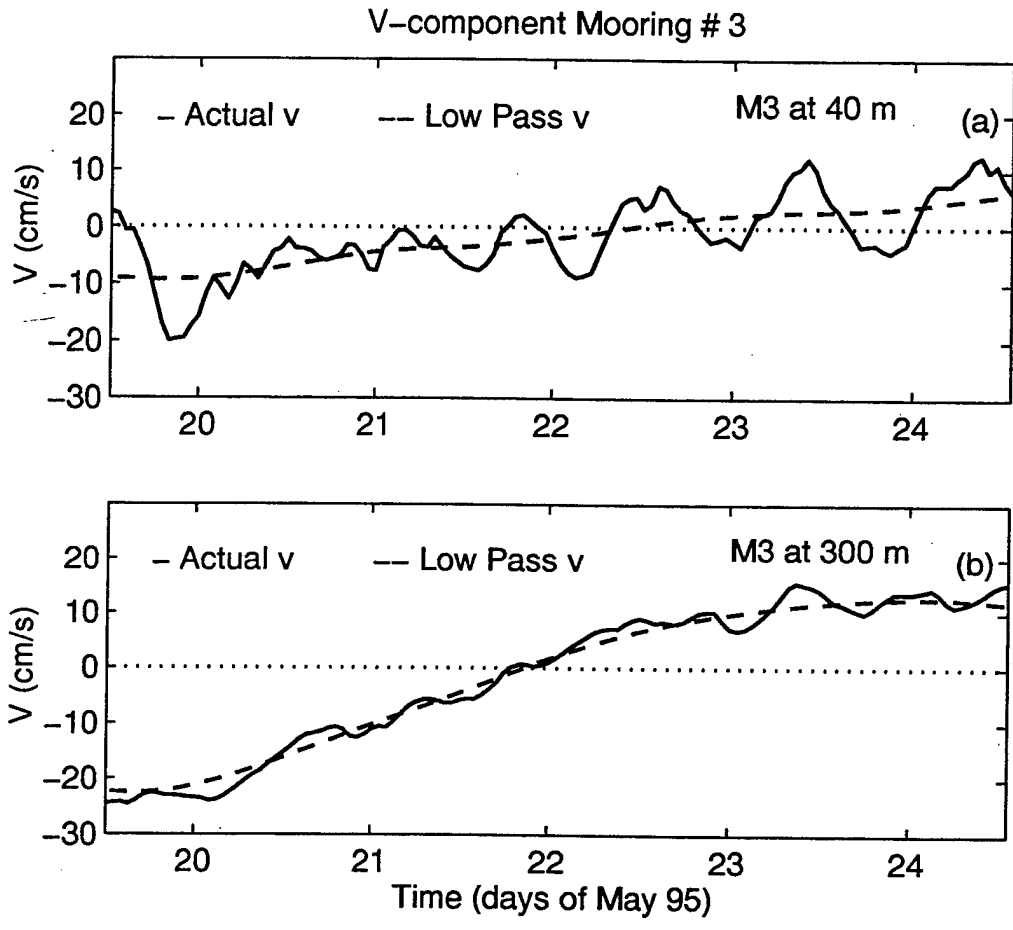


Figure 22: Raw (actual) and low pass filtered currents at mooring M2 for two depths, 50 m (a), 300 m (b).

In order to conduct a meaningful comparison between the geostrophically-derived currents and the results of the previous section, segments of the low pass north (v) component of the mooring velocity time series were selected and time averaged. The time period used for the averaging process was the period of the CTD casts of the stations located in the vicinity of the moorings.

Figs. 23, 24 and 25 show these averaged velocities at the cross-sections near M2-M6, M7 and M8. Table II presents the hydrographic stations and the time periods that were used to perform the averaging.

The comparison of the two flow fields is discussed in the next Chapter.

Table II: Moorings, CTD stations nearby the moorings, time period used for the current averaging process.

Mooring #	Stations involved	Time Period - May 95 (DDHH)
M2	Magnaghi 003,004,005	2009 - 2012
M3	Magnaghi 002,003	2007 - 2010
M4	Alliance 004,005	2002 - 2006
M5	Alliance 001,002,004	1923 - 2004
M6	Alliance 001,002	1921 - 1923
M7	Magnaghi 046 and Alliance 053,054	2300 - 2305
M8	Urania 023,024,025	2401 - 2405

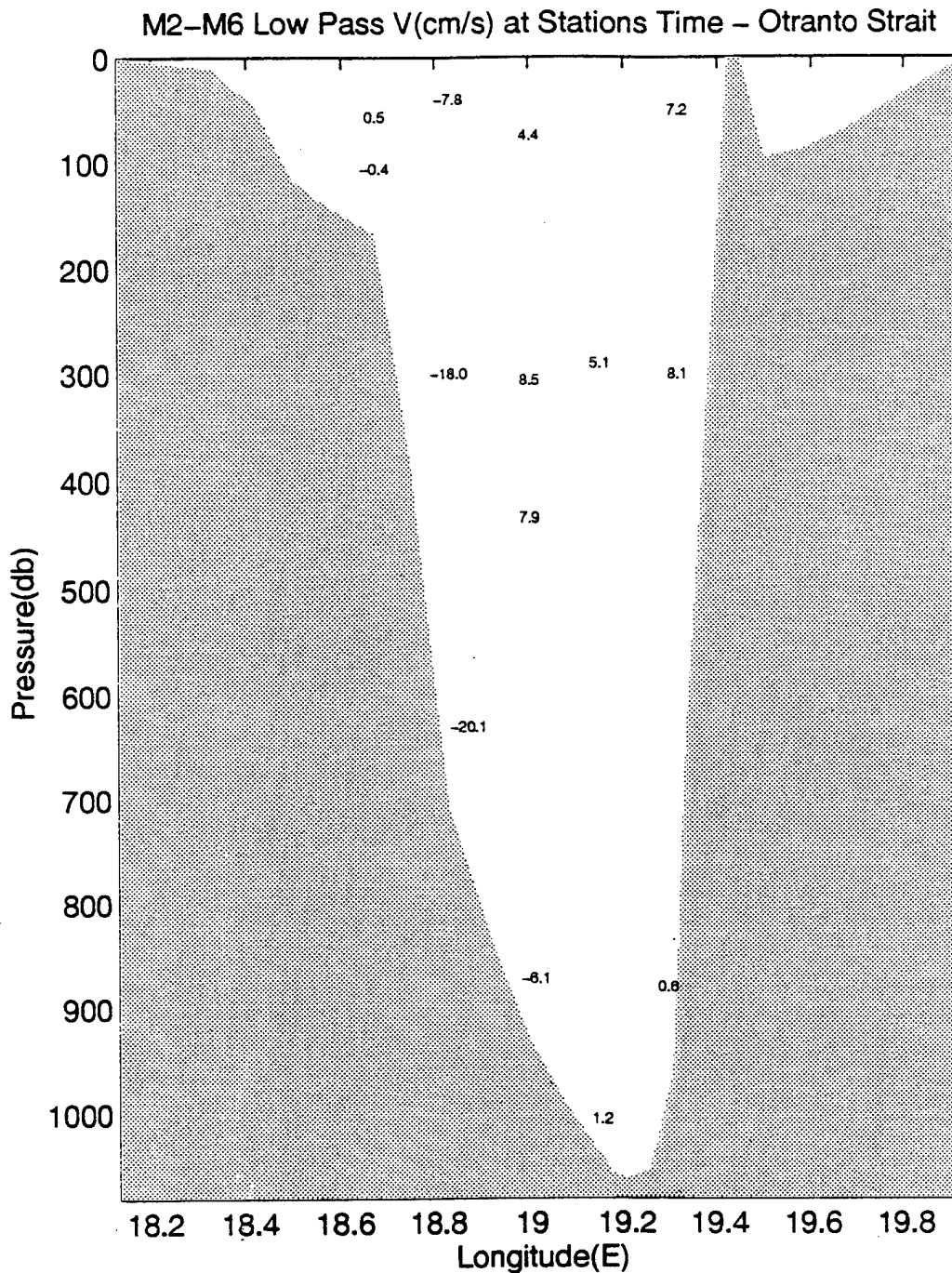


Figure 23: Average of the low pass northward velocity ( $v$ ) at the current meter location for moorings M2 to M6. The average was taken over the time period at which nearby CTD stations were occupied (see Table II). Positive values indicate northward flow.

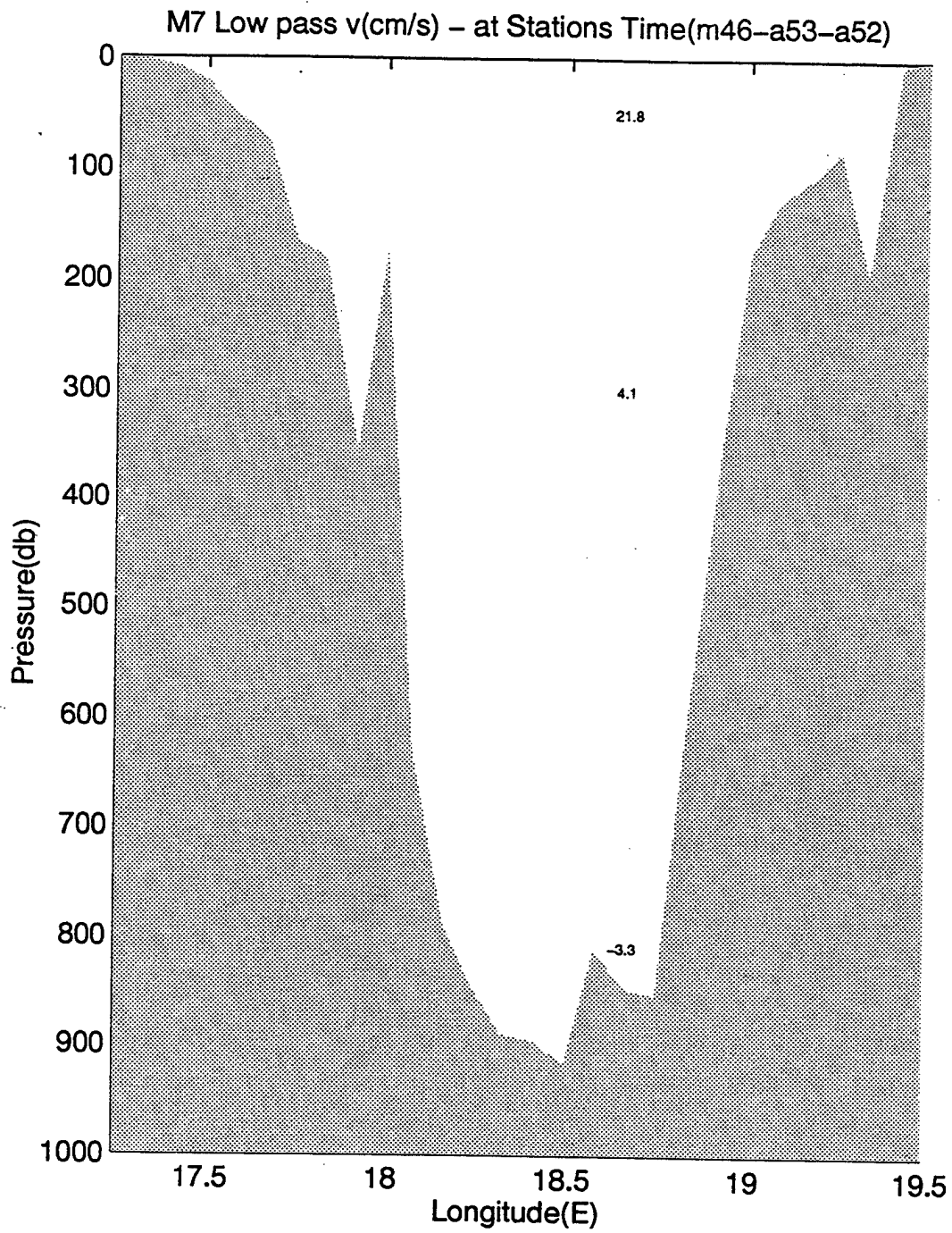


Figure 24: Same as Figure 23 but for mooring M7.

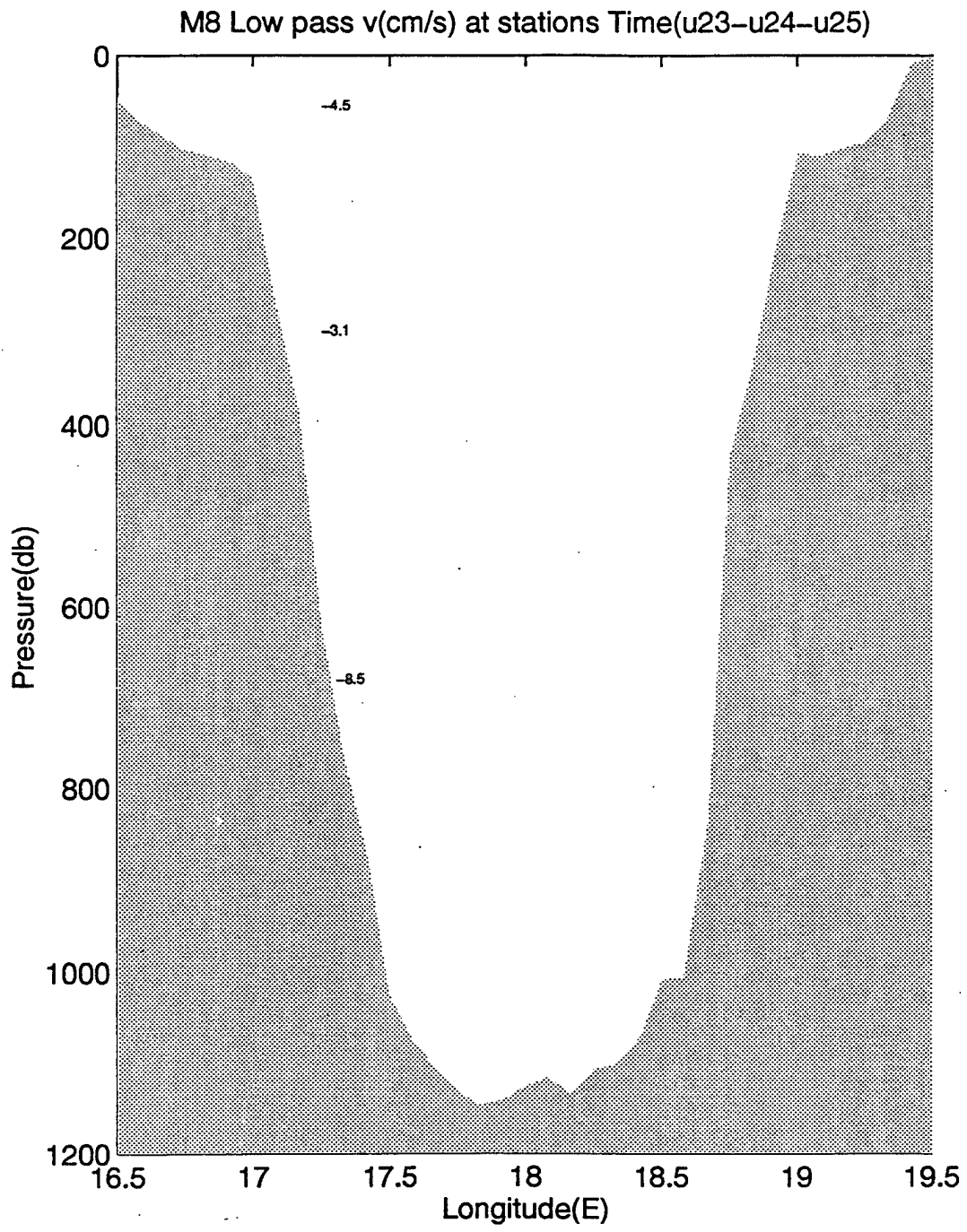


Figure 25: Same as Figure 23 but for mooring M8.

## 2. Moored Current Meter Velocities and Drifter Paths

Further analysis of the circulation pattern involves the comparison of the drifter paths and the velocity vectors obtained from the u and v components of the current meter data. Figs. 26 to 27 show the drifter trajectories for the period of the cruise (19-24 May 1995). The thick arrows represent the moored current meter velocity vectors near a depth of 50 m. The small solid circles indicate the drifter positions at 00 UT on each day. Thin paths are the trajectory tails going back in time for a maximum of 5 days. They indicate the direction and speed of the drifter motion.

From the analysis of such plots for the period of the cruise, we note a relatively steadiness for the area north of  $41^{\circ}\text{N}$ . The directions change slowly and the magnitudes remain almost constant. This is additional evidence that the flow north of  $41^{\circ}\text{N}$  evolves slowly and, as a consequence, is more in geostrophic equilibrium. South of  $41^{\circ}\text{N}$  the behavior is rather unsteady. Both the drifters and the current meter vectors that were heading north, east of  $19^{\circ}\text{E}$ , changed direction on 20 May and subsequently head south on 22-24 May. As noted before, this change in direction is coupled with the change in wind direction on the eastern side of the Otranto Strait. West of  $19^{\circ}\text{E}$ , the M2 currents increase in magnitude from approximately 0 cm/s on May 20 to approximately 10 cm/s southward on May 22. The currents at M3 changed both in direction and magnitudes approximately 10 cm/s southward on May 20 to approximately 5 cm/s northward on May 24.

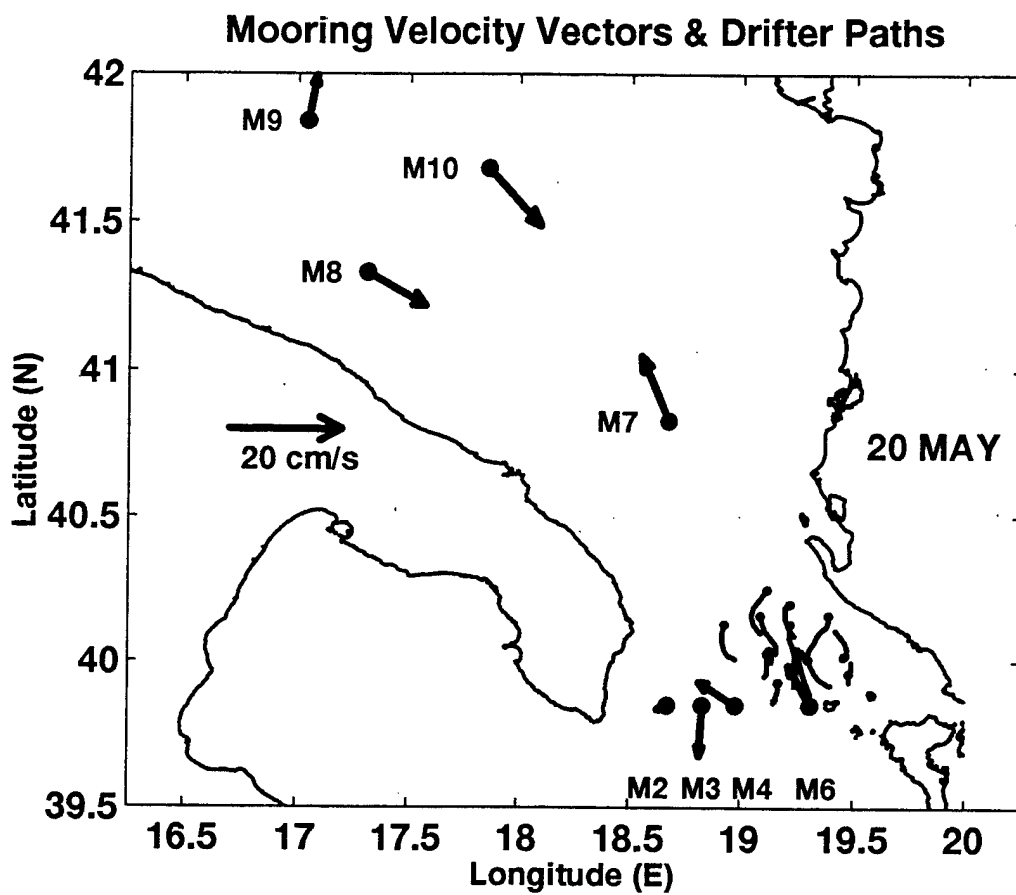


Figure 26: Thick arrows represent moored current vectors at approximately 50 m for May 20; thin paths represent a maximum of 5 days of drifter track (beginning on 19 May).

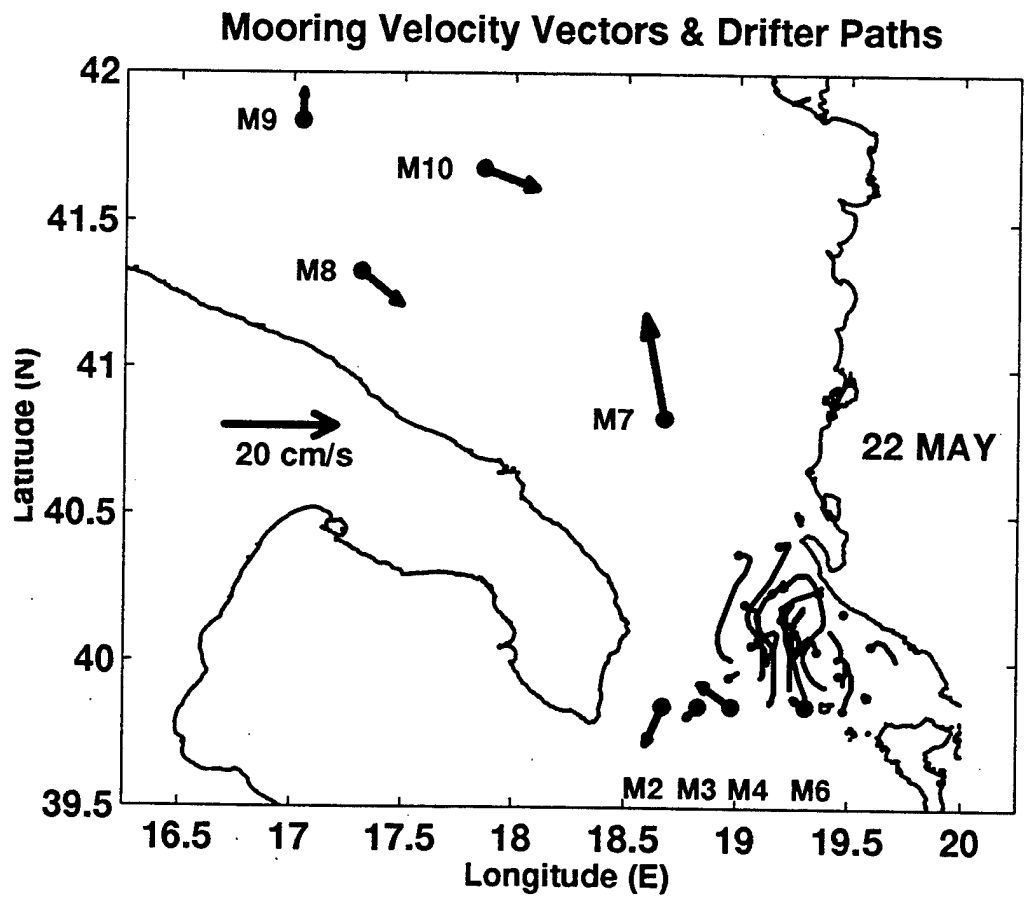


Figure 27: Same as Fig. 26 but on May 22.

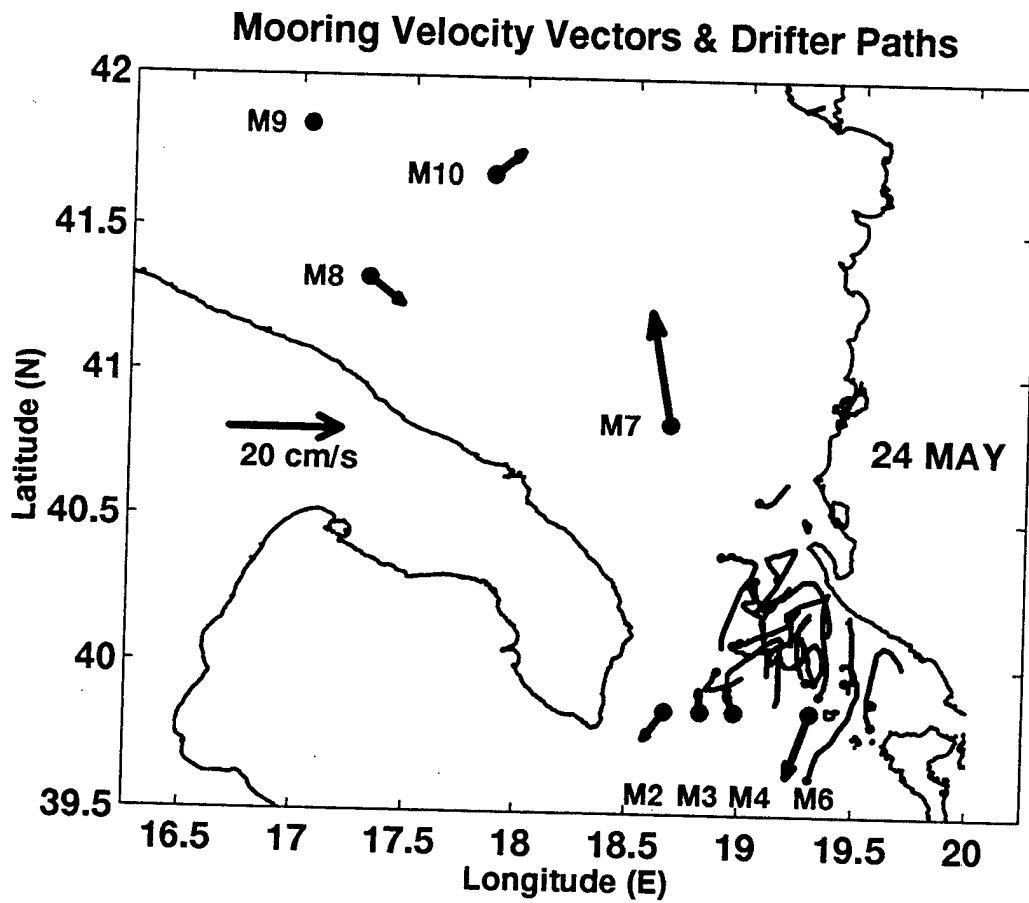


Figure 28: Same as Fig. 26 but on May 24.

## VI. DISCUSSION

In this Chapter we discuss and compare the results presented in the previous Chapter. A qualitative comparison is made between the relative geostrophic maps, the P-vector results and the directly measured currents by moored current meters, drifters, and shipborne ADCP. In section A, we discuss the horizontal sections at 40 and 200 m and relate them to the mooring velocity vectors and to the drifter tracks (Figs. 23 to 25). The first depth, 40 m, is representative of the surface waters (see Fig. 2). At 200 m (average depth for the MLIW core flowing into the Adriatic) we anticipate a significant flow in the northward direction. Both maps will be compared qualitatively with ADCP plots and with a clear thermal satellite image of the area in section C. In section B selected vertical cross-sections are compared. Cross-sections of the northward absolute geostrophic currents obtained by the P-vector calculations at the latitudes of the moorings M2-M6, M7 and M8 are compared with the averaged low pass velocity component of the moored current meter data. In addition, we present and discuss the mooring-derived and the geostrophic vertical shears.

### A. P-VECTOR ABSOLUTE GEOSTROPHIC FLOW AND MOORING VELOCITIES

As mentioned in Chapter V, the synopticity of hydrographic data, mainly at the Otranto Strait, is a crucial factor in intercomparing data sets or analysis methods. The current meter and the wind data (Figs. 21 and 22) disclose clearly a change in the circulation regime mainly caused by a wind reversal on 21 May, half way through the survey. The comparison between the geostrophic currents and the direct measured velocity estimates have to be made "locally", that is, the direct velocity measurements have to be considered during the time period at which the CTD casts were made in the vicinity of the moorings.

For this area a synoptic period can be considered as the one were the flow, as depicted by the drifters and the mooring velocity vectors, do not show a significant change. This happens from 19 to 21 May when the Otranto Strait area was surveyed. For the southern Adriatic area, the measurements can be considered synoptic between 22 and 24 May.

At the Otranto Strait area, the 40 m horizontal sections (Figs. 13 and 16) show that the flow is northwards east and west of  $19^{\circ}$  E, and that an outflow is evident near that longitude. The northward flow east of  $19^{\circ}$ E agrees relatively well with the drifter and mooring results for the period 19-21 May (Figs. 26 and 27) as far north as approximately  $40.5^{\circ}$ N. At 200 m we do not see a significant northward flow in the geostrophic flow maps, as might be expected by examining the salinity horizontal section (Fig. 12 middle panel) where the influence of the MLIW as far north as  $41.5^{\circ}$ N is clearly seen. The flow is rather weak and seems to be dominated by mesoscale circulation patterns (Gacic et al., 1996).

Near the locations of moorings M7 and M8 in the southern Adriatic the qualitative agreement is much better due the greater steadiness of the circulation. The directions are roughly the same, but the magnitudes of absolute currents are small. In this area a cyclonic flow is present north of  $41^{\circ}$  N. This is consistent with the observations of Orlic et al. (1992). The same cyclonic flow, although, not so clear, is evident at the 200 m level (Figs. 14 and 17).

#### **B. P-VECTOR NORTHWARD ABSOLUTE GEOSTROPHIC FLOW VERSUS NORTHWARD CURRENT METER VELOCITIES**

The P-vector method was performed along 21 cross-sections in latitude. Each one of them is located between pairs of 22 latitudes of the regular grid used to contour the data. The average between cross-sections 21 ( $39.75^{\circ}$  N) and 20 ( $39.80^{\circ}$ N) was

used for comparison with the M2-M6 mooring array. The average cross-sections between 07 and 08 (41.15 °N) were compared to M7 and finally the average cross-sections between 02 (41.45 °N) and 03 (41.40 °N) were compared to M8. The moored current meter v-component low pass filtered data were averaged using the same time period as the nearby CTD casts (see Table II).

Figs. 18 and 23 show, respectively the cross-section of the v-component absolute geostrophic flow as deduced by the P-vector method at the latitude of M1-M6 and the averaged v-component velocities for the above moorings when the nearby CTD stations were occupied. Comparing the results we see that the direction is correct for M2 and M6 at the surface (approx. 50 m), for M3 and M5 at mid depth (approx. 300 m) and for M3 near the bottom (approx. 650 m). In all these cases, the magnitudes are however different, the P-vector estimates being as low as 5% than the current meter velocities. For the other moorings and depths, no agreement can be found.

The same analysis made at mooring the M7 latitude shows good agreement in the flow direction for the near-surface (approx. 50 m) and mid-level depths (approx. 300 m). In this case the magnitudes of the P-vector estimates are about 50% less than the directly measured speeds. Near the bottom the P-vector significantly underestimate the actual current speeds.

For mooring M8, the directions are correct at the surface and at the bottom and opposite at mid depth. The geostrophic magnitudes are decidedly too small throughout the water column (about 10% of the direct estimates).

In order to check the geostrophic assumption, the balance between the pressure gradient and Coriolis forces (a necessary condition for the application of the P-vector method), the vertical geostrophic shear between the depths of the current meters was calculated using the CTD stations data (not with the interpolated gridded values). Table II shows the stations used

for the calculation of the vertical geostrophic shears, and the time periods used for averaging the current meter low pass filtered northward velocities. Table III presents the comparison between the mooring and geostrophic shears.

Table III: Mooring current meter and geostrophic shears (cm/s).

MOORING #	Shear between(m)	Mooring	Geostrophic
2	50-100	0.9	0.46
3	50-300	10.2	5.9
4	74-306	-4.1	-1.1
	306-434	0.6	-0.20
	434-872	14.0	-11.95
5	300-1020	-3.9	-0.85
6	50-300	-0.9	6.8
7	50-300	17.7	5.59
	300-810	7.4	-
8	55-300	-1.4	-0.97
	300-680	5.4	-

In the near-surface layers (approx. 50-300m) relatively small departures are found for moorings M2, M3 and M8 with the geostrophic shear being more than 50% of the mooring shear. At these locations the flow appears to be more geostrophic. This could be the reason for the relative good results of the P-vector method at the surface layers compared to the drifter and mooring vectors at 50 m on 20 May (Fig. 26). On the other hand the difference is quite substantial for moorings M4 and M7 where the mooring shear difference can be 4 times larger than the geostrophic shear. For the deepest layer (approximately 300-900m), the mooring and the geostrophic shears can even be of

opposite sign. The results above show that, in general, the departure from geostrophy at the Otranto Strait, is rather high, except for the near surface layer.

To assess the causes for this ageostrophy, we need to estimate the magnitudes of the acceleration term ( $du/dt$  and  $dv/dt$ ), the Coriolis term ( $f*u$  and  $f*v$ ) and the advection term ( $\mathbf{v} \cdot \nabla \mathbf{v}$ ) in the horizontal equation of motion.

From the current meter velocity time series (Figs. 21 and 22) we can estimate the acceleration,  $dv/dt$ . Using the worst case with maximum acceleration, i.e., the velocity at 300 m of mooring M3 (see Fig. 22), we obtain:

$$|\Delta v| = 20 \text{ cm/s,}$$

$$|\Delta t| = 2 \text{ days} = 2 * 24 * 3600 \text{ sec} = 172800 \text{ sec,}$$

$$|\Delta v / \Delta t| = 1.15 \times 10^{-4} \text{ cm/s}^2.$$

Using typical values for the Coriolis parameter, flow speed and horizontal scale ( $f = 10^{-4} \text{ s}^{-1}$ ;  $v = 10 \text{ cm/s}$  and  $L = 10 \text{ km}$ ), we estimate the following orders of magnitude:

$$f*u = 10^{-4} * 10 = 10^{-3} \text{ cm/s}^2,$$

$$\mathbf{v} \cdot \nabla \mathbf{v} \sim (v^2/L) = 10^2/10^5 = 10^{-3} \text{ cm/s}^2.$$

From the estimations above we see that it is the advection term (same order of magnitude as the Coriolis term) that is one of the major causes for the ageostrophic behavior. Another obvious cause is the wind stress at the surface that can create significant wind-driven currents.

A possible explanation for the ageostrophy in the surface layers is in terms of the conservation of vorticity in the

Strait. In the vicinity of the sill (Fig. 2), we observe that water entering the Adriatic and crossing the sill experiences two simultaneous effects: first, it tends to stretch out (the column of water, after crossing the sill, increases), and this generates cyclonic vorticity. In second place, the water tends to diverge which in turn generates anti-cyclonic vorticity. The opposite happens with the outward flow on the other side of the strait. These opposite effects in the vorticity end up making the local rate of change in the vorticity,  $\partial\zeta/\partial t$ , small. The simplified vorticity equation is :

$$\begin{aligned} \partial\zeta/\partial t + \mathbf{v}\cdot\nabla\zeta &= f\partial w/\partial z + 1/\rho(\partial/\partial z(\partial\tau_y/\partial x - (\partial\tau_x/\partial y)) \end{aligned} \quad (11)$$

(a)      (b)      (c)      (d)

where the twisting<sup>(1)</sup>, vertical vorticity advection,  $\beta v$  and friction terms were assumed to be small.  $\zeta$  is the relative vorticity,  $f$  is the Coriolis parameter,  $w$  is the vertical velocity,  $\rho$  is density and  $\tau_x$  and  $\tau_y$  are the wind stress components. The above equation is derived taking the curl of the "x" and "y" momentum equations:

$$\begin{aligned} du/dt + u\cdot\nabla u + w\partial u/\partial z &= fv', \end{aligned} \quad (12)$$

(e)

$$\begin{aligned} dv/dt + v\cdot\nabla v + w\partial v/\partial z &= fu', \end{aligned} \quad (13)$$

(f)

1. It is recognized that the twisting term has the potential to be significant near steep topography, like the Otranto sill, where  $w$  ( $z$  component of the velocity vector  $\mathbf{V}$ ), can be large over a small horizontal scale. This could be studied in the future.

where  $u'$  and  $v'$  are the ageostrophic components of  $u$  and  $v$ . If  $\partial\zeta/\partial t$ , is approximately zero in equation (11), the relative vorticity advection (b) (which comes in part from the advection of both the  $u$  (e) and  $v$  (f) components of eqs. (12) and (13)), has to balance the vertical stretching term (c) and the wind stress curl (d).

This means that, assuming the local change of vorticity is near zero, any advection (north or south) plus any significant wind stress curl, again north or south, will result in a rebalancing of equation (11). Depending on the sign and magnitude of the new terms (b), (c) and (d) the ageostrophic velocities  $u'$  and  $v'$  in (12 and (13) will be changed in response to this new balance.

### C. P-VECTOR ABSOLUTE GEOSTROPHIC CURRENTS VERSUS ADCP AND AVHRR MAPS

The results of the OGEX1 ADCP data are shown in Figs. 29 and 30. The velocity vectors are plotted along the sections made by the NRV Alliance (Fig. 3). The plots show a rather weak flow, as should be expected in spring in the Otranto Strait and Southern Adriatic areas. The circulation is dominated by small scale features at both 50 and 200 m. Comparing the ADCP current maps with the geostrophic maps at 40 and 200 m (Figs. 13 and 17), we find qualitative agreement for the flow directions, however, the P-vector results have magnitudes about 50% smaller with respect to the ADCP currents. As pointed out above, the ADCP data measures the total velocity i.e., both the geostrophic and the ageostrophic components. The latter are not considered in the P-vector calculations. This comparison suggests the ageostrophic and geostrophic components are of approximate equal magnitudes.

The AVHRR image of 23 May at 17:14 UT (Fig. 28) shows very distinctly the distinction between the relatively warm waters

(ISW, in orange-reddish color) and the relatively cold ones (ASW, in bluish color). The ISW spans from the Ionian basin (lower portion of the image) into the Adriatic Sea as far north as 41 °N. The major body of the ISW is concentrated on the eastern portion of the image. The ASW is evident on the western portion of the map. In addition, relatively cold waters are also evident as a consequence of upwelling (at the time of the image the wind had been blowing southward for at least 2 days). The upwelling events can be seen on the Albanian coast (dark blue from approximately 40 °N to 40.4 °N) and on the west coast of Corfu Island (dark blue south of 39.5°N).

As a consequence of the upwelling, a tongue of cold water can be seen south of the Albanian upwelling area progressing southward opposite to the inflow of the ISW. The south-southwestward movement of the tongue is also very well depicted by the drifter displacements overlaid on the thermal image. Solid dots represent the drifter location at the time of the image and the attached tail represents the displacement during the previous 11 hours.

A noteworthy mesoscale feature is evident near 41°N and 18.67°E in the geostrophic maps, the ADCP current field and in the surface thermal image. It is a surface intensified anti-cyclone eddy structure associated with the relatively warm and fresh water originating from the Albanian rivers. The "mushroom" shaped feature in the AVHRR image (Fig. 31) shows its connection to the shelf water and its tendency to to expand on the shelf and eventually pinch off.

In conclusion, we can state that the P-vector method is not useful in coastal areas where the flow can be substantially ageostrophic. The method works better in the open southern Adriatic, but the results are similar to the relative geostrophic flow maps using a deep reference layer.

**OGEX1**  
19-24 May 1995

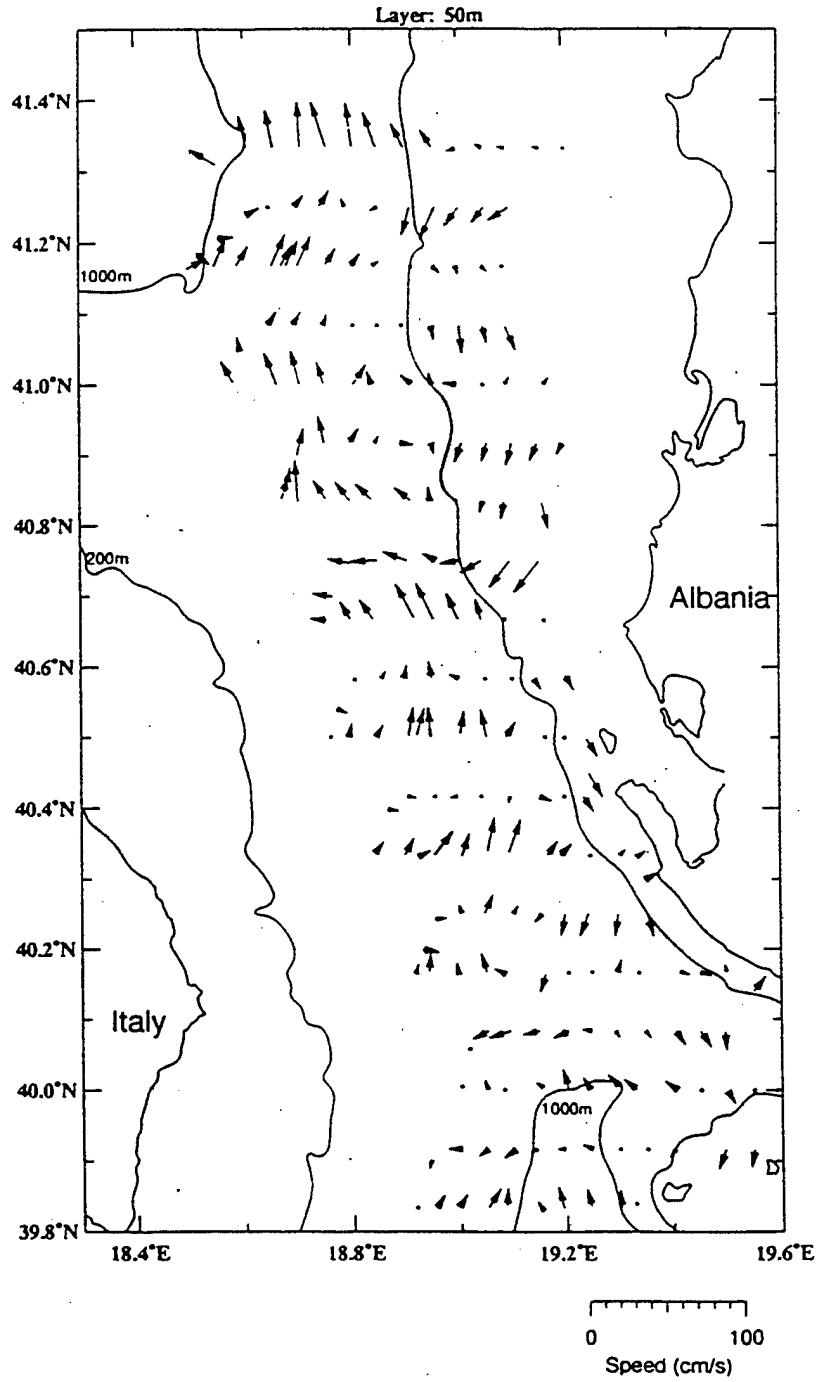


Figure 29: ADCP velocity vectors at 50 m (from Brauns, 1997).

# OGEX1

19-24 May 1995

Layer: 200m

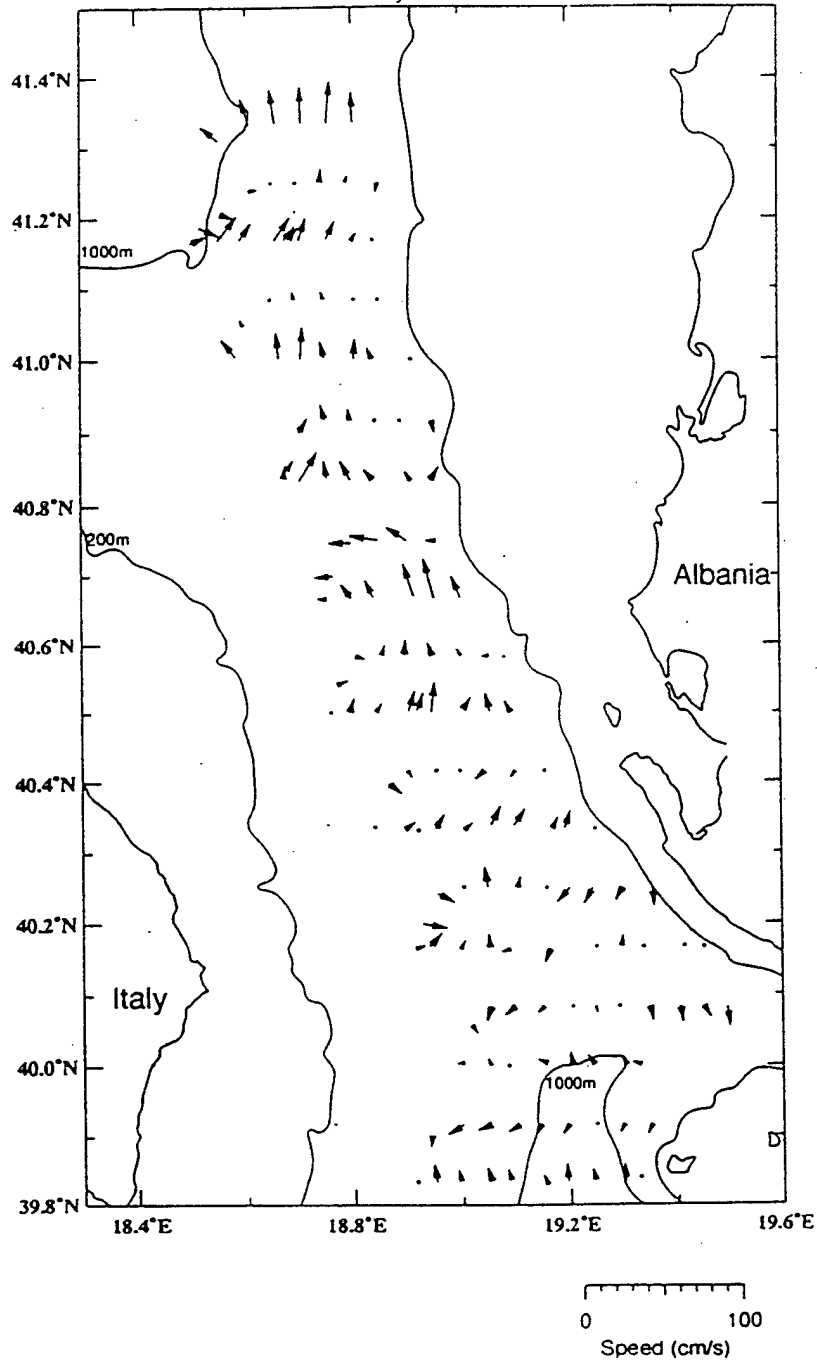


Figure 30: Same as Fig 30 but at 200 m (from Brauns, 1997).

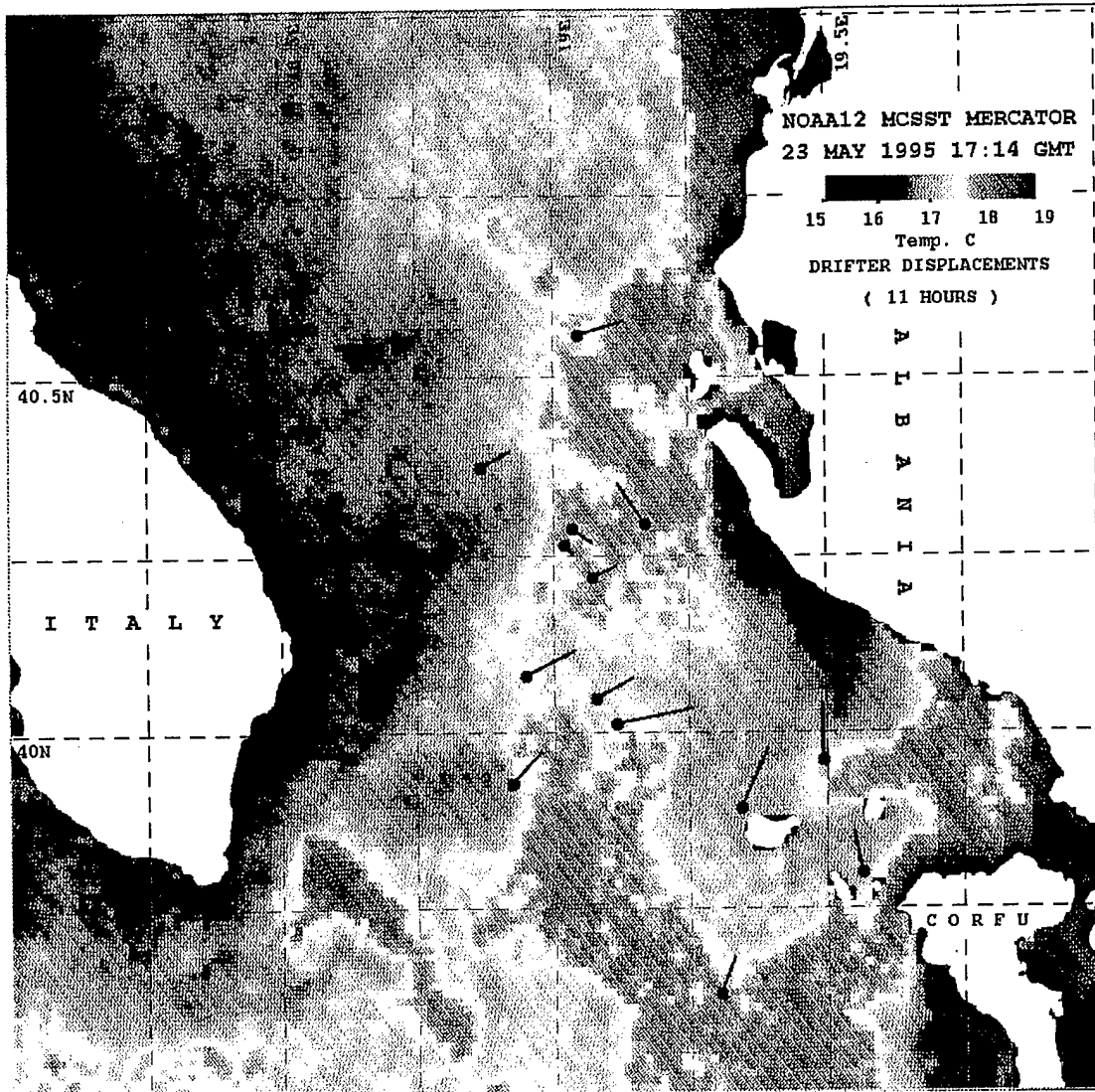


Figure 31: Satellite (AVHRR) image taken on 23 May 1995 of the Otranto Strait and Southern Adriatic. Sea surface temperatures are color-coded. Surface drifter displacements are overlaid on the image. Solid dots represent the drifter position at the time of the image. The attached tails represents the displacement during the previous 11 hours.

## VII. CONCLUSIONS AND RECOMMENDATIONS

### A. CONCLUSIONS

As part of the Otranto Gap project, the NATO Undersea Research Centre (SACLANTCEN) carried out the OGEX1 cruise with main focus on the oceanography of the Otranto Strait and the southern Adriatic regions. OGEX1 included hydrographic surveys, moored current meter and drifter deployments. The hydrographic data were used to study the water masses and were utilized as an input for the estimation of the absolute geostrophic velocity field via the P-vector method. The results of the latter were in turn compared with the directly measured velocities from the drifters and moored current meters.

Our conclusions are:

1. Although less strong than in winter, the inflow of MLIW water was clearly observed in the T-S diagrams (Figs. 8 and 9) and in the vertical and horizontal T, S and Sigma-t sections (Figs. 10 and 11) in May 95. The MLIW flows along the Albanian coast and its core is at about 180 m depth. The influence of Albanian rivers is also observed as a relatively warm and fresh tongue (Fig. 12, top and middle panels), and in the AVHRR image as a "mushroom" shaped anti-cyclone (Fig. 31). Along the western coast the water is rather fresh confirming the influence from the Po River runoff, flowing south along the Italian coast.

2. The wind was shown to exert a major contribution on the circulation in the Adriatic. In Fig. 21 (a) and (b), we see the response of the near surface currents to the wind forcing. The same wind can also cause upwelling events (Fig. 31) on the eastern coast of the Adriatic. As a consequence, south-southwestward tongues of cold water tend to oppose the ISW inflow.

3. The P-vector method can be used as a first approximation for estimating the absolute velocity field in the southern

Adriatic north of  $41^{\circ}$  N. The area is in relatively steady state and the geostrophic balance, to a certain extent, is valid. The cyclonic gyre around the South Adriatic Pit was confirmed by the P-vector calculations, the relative geostrophic flow maps and the other current measurements.

4. At the Otranto Strait, the results of the P-vector field method need to be interpreted with caution. The area was shown to be very ageostrophic. The direct measured velocity shears are, in general, substantially greater than the geostrophic ones (Table III). The horizontal advection and friction (near the bottom) are the major causes for the ageostrophy. Only for the near-surface layer, which appears more geostrophic, is there some qualitative agreement between the drifter, current meter and P-vector results.

## B. RECOMMENDATIONS

1. We recommend to be very cautious when applying the P-vector method in coastal or semi-enclosed sea areas because the complex dynamics generally make the flow quite ageostrophic.

2. We recommend the use of the DFI (Digital Filter Initialization) with the same data set used in this thesis, to produce a dynamically balanced 3D velocity field. The DFI technique (see Viudez et al., 1996, for its application in the Alboran Sea), integrates forward and backward the absolute velocity field as obtained by a quasi-synoptic T and S (density field) data set, using a PE ocean model. The results are then plotted against time and time averaged. The averaging uses a weighting function based on a low pass digital filter. This procedure filters out the high frequency oscillations in the time series, caused by the imbalanced initial state. It tends to generate a dynamically balanced three-dimensional density or velocity field, which in turn can be used as an initial condition for ocean models.

3. The three-dimensional absolute geostrophic currents estimated by the P-vector in the open southern Adriatic could be used as boundary and initial conditions for ocean models. The absolute field, although not really true, is better than assuming zero velocities.



## LIST OF REFERENCES

Artegiani A., M. Gacic, A. Michelato, V. Kovacevic, A. Russo, E. Paschini, P. Scarazzato and A. Smircic, The Adriatic Sea Hydrography and Circulation in Spring and Autumn (1985-1987), Deep-Sea Research II, 40 (6), 1143-1180, 1993.

Brauns, B., Adriatic Sea Current Observations using Acoustic Doppler Current Profiler (ADCP), Master's Thesis, Naval Postgraduate School, Monterey CA, 1997.

Buljan, M., and M. Zore-Armanda, Oceanographical Properties of the Adriatic Sea, Oceanogr. Mar. Biol. Ann. Rev., 14, 11-98, 1976.

Chu, P., P-Vector Method for Determining Absolute Velocity from Hydrographic Data, MTS Journal, 29 (2), 3-14, 1995.

Gacic, M., V. Kovacevic, B. Manca, E. Papageorgiou, P.-M. Poulain, P. Scarazzato and A. Vetrano, Thermohaline Properties and Circulation in the Otranto Strait, Bulletin de L'Institut Océanographique, Monaco, CIESM Sciences Series 2, Special volume 17, 117-145, 1996.

Killworth, P. D., A Bernoulli Inverse Method for Determining the Ocean Circulation, J. Phys. Oceanogr., 16, 2031-2051, 1986.

Neddler, G. T., The Absolute Velocity as a Function of Conserved Measurable Quantities, Prog. Oceanogr., 14, 421-429, 1985.

Ovchinnikov, I. M., V. I. Zats, V. G. Krivosheya and A. I. Udodov, A Forming of Deep Eastern Mediterranean Water in Adriatic Sea (in Russian), Okeanologiya, 25 (6), 911-917, 1985.

Orlic, M., M. Gacic, and P. E. La Violette, The Currents and Circulation of the Adriatic Sea, *Oceanol. Acta*, 15, 109-124, 1992.

Poulain, P.-M., OGEX1 Cruise Report, Internal Report, SACLANT Undersea Research Centre, La Spezia, Italy, May 1995.

Poulain, P.-M., Current Measurements in the Strait of Otranto Reveal Unforeseen Aspects of its Hydrodynamics., *EOS, Trans., American Geophysical Union*, 20 (36), 345-348, 1996.

Poulain, P.-M., Drifter Observations of the Surface Circulation in the Adriatic Sea between December 1994 and March 1996, *J. Mar. Sys.*, 1998, in press.

Poulain, P.-M., and P. Zanasca, Drifter and Float Observations in the Adriatic Sea (1994-1996), Data Report, SM-340 SACLANT Undersea Research Centre, La Spezia, Italy, 1998, in press.

Stommel, H., and M. S. Schott, The Beta Spiral and the Determination of Absolute Velocity Field from Hydrographic Station Data, *Deep-Sea Res.*, 24, 325-329, 1977.

Thompson, R. O. R. Y., Low-pass Filters to Surpass Inertial and Tidal Frequencies, *J. Phys. Oceanogr.*, 13, 1077-1083, 1983.

Viudez, A., R. Haney, and J. Tintoré, Circulation in the Alboran Sea as Determined by Quasi-Synoptic Hydrographic Observations. Part II: Mesoscale Ageostrophic Motion Diagnosed through Density Dynamical Assimilation, *J. Phy. Oceanogr.*, 26 (5), 1996.

Wunsch, C., and B. Grant, The General Circulation of the North Atlantic West of 50° W Determined from Inverse Methods, Rev. Geophys., 16, 583-620, 1978.

Zoccolatti L. and E. Salusti, Observations of a Vein of Very Dense Marine Water in the southern Adriatic Sea, Continent. Shelf Res., 7, 535-551, 1987.

Zore, M., On Gradient Currents in the Adriatic, Institute of Oceanography and Fisheries, 6 (6) 1-40, 1956.

Zore-Armanda, M., Mixing of Three Water Masses in the South Adriatic, Rapp. P. -v. Reun. Commn. Int. Explor. Scien. Me. medit., 17(3), 879-885, 1963.



INITIAL DISTRIBUTION LIST

1. Defense Technical Information Center . . . . . 2  
8725 John J. Kingman Rd., STE 0944  
Ft. Belvoir, VA 22060-6218
  
2. Dudley Knox Library . . . . . 2  
Naval Postgraduate School  
411 Dyer Rd.  
Monterey, CA 93943-5101
  
3. Professor Robert Bourke . . . . . 1  
Code OC/BF Dept Oceanography  
Naval Postgraduate School  
833 Dyer Rd. Rm. 328  
Monterey, CA 93943-5122
  
4. Professor Pierre Poulain . . . . . 5  
Code OC/PN Dept Oceanography  
Naval Postgraduate School  
833 Dyer Rd. Rm. 328  
Monterey, CA 93943-5122
  
5. Professor Peter Chu . . . . . 1  
Code OC/BF Dept Oceanography  
Naval Postgraduate School  
833 Dyer Rd. Rm. 328  
Monterey, CA 93943-5122
  
6. Director . . . . . 1  
SACLANT Undersea Research Centre  
SACLANTCEN CMR\_426  
APO-AE 09613-5000

7. CT(T) RENATO LIMA PINTO . . . . . 2

Diretoria de Hidrografia e Navegação

Rua Barão de Jaceguay s/n

24000 - Niterói - RJ.

Brasil